PROBABILISTIC TSUNAMI HAZARD ANALYSIS FOR TUZLA TEST SITE USING MONTE CARLO SIMULATIONS

by

Hafize Basak Bayraktar

B.S., Geophysical Engineering, Istanbul University, 2012

Submitted to Kandilli Observatory and Earthquake Research Institute
in partial fulfillment of the requirements for the degree of
Master of Science

Graduate Program in Geophysics

Boğaziçi University

2018

ACKNOWLEDGEMENTS

First of all, I am extremely grateful to my co-advisor Dr. Ceren Özer Sözdinler for her endless support, encouragement and supporting guidance. I am hugely indebted to her for spending limitless hours and inspiring instruction in the development and completion of my study.

I would like to express my sincere thanks to my advisor Prof. Dr. Hayrullah Karabulut for his guidance and sharing his valuable knowledge with me during my studies.

I would like to specially thank to Prof. Dr. Ahmet Cevdet Yalçıner for his valuable feedback and effort during this study and great support of Bora Yalçıner and Andrey Zaitsev in the development of the NAMI DANCE numerical code.

I would like to thank to Deniz Ertuncay, Esra Kalkan,Figen Eskiköy and Pınar Büyükakpınar for their valuable friendship,patience, support and encouragement at the every stage of my study and my life.

I also would like to acknowledge Dr. Öcal Necmioğlu, Prof. Dr. Semih Ergintav, Prof. Dr. Sinan Akkar, Dr. Mine Demircioğlu and Prof. Dr. Mustafa Erdik for their valuable help, patiently explanations and guidance to improve my thesis.

Last but not least, I must express my very profound gratitude to my husband Oğuz Bayraktar, my parents Sevgi and Gürsel Fırat and all other members of my family for providing me with unfailing support and continuous encouragement throughout my years of study and through the process of researching and writing this thesis. This accomplishment would not have been possible without them.

ABSTRACT

PROBABILISTIC TSUNAMI HAZARD ANALYSIS FOR TUZLA TEST SITE USING MONTE CARLO SIMULATIONS

In this study, time-dependent probabilistic tsunami hazard analysis (PTHA) is performed for Tuzla in the Sea of Marmara, Turkey, related to the possible rupture of Prince Island Fault within next 50, 100, 500 and 1000 years. The study associates the probabilistic seismic hazard analysis with tsunami numerical modelling. Synthetic earthquake catalogue, which includes 100 events, was generated by Monte Carlo (MC) simulation technique. This catalogue includes earthquakes having magnitudes between Mw 6.5 and 7.1 (that comes from the maximum moment magnitude range this fault system can generate), of which probability of occurrence and associated tsunami wave heights are calculated. Tsunami numerical code NAMI DANCE using Non-Linear Shallow Water Equations are used for tsunami simulations. According to results of the tsunami numerical modelling, distribution of probability of occurrence with respect to minimum and maximum water surface elevations and maximum flow depth on land are represented. Moreover, tsunami inundation maps of Tuzla region are prepared with regard to probability of exceedance of 0.3 m flow depth and probability of exceedance of 0.3 m tsunami wave heights at synthetic gauge points for different time scales. This was observed that tsunami wave heights up to 1 m have 65% probability of exceedance for 50 years return period and this value reaches up to 85% in Tuzla region for next 100 year. Inundation depth also exceeds 1m in Tuzla region with probabilities of occurrence of 60% and 80% for next 50 and 100 years, respectively. When return period increases by 500 and 1000 years, earthquake occurrences demonstrate very high probabilities. Furthermore, inundation maps show that the probability of occurrence

of certain flow depths ranges between 10% and 75% when exceedance threshold of wave height considered as 0.3 m for 50 and 100-year time exposure. The maximum inundation distance calculated among entire earthquake catalogue is 60 m in this test site. Looking at the situation for the synthetic gauge points, only few of them has a probability between 75% - 85% when probability of exceedance of 0.3 m wave height is considered for next 50 years and this probability value increases up to 90% for 100-year exposure time. Probabilities are observed more than 95% for 500 and 1000-year return periods due to the short return periods of characteristic faults in Marmara Sea.

ÖZET

TUZLA ÇALIŞMA ALANI İÇİN MONTE CARLO SİMÜLASYONU İLE OLASILIKSAL TSUNAMİ TEHLİKE ANALİZLERİ

Bu çalışmada, Prens Adaları Fayı'nın 50, 100, 500 ve 1000 yıl içerisinde kırılması durumunda, Tuzla'da oluşacak zamana bağlı olasılıksal tsunami tehlike analizleri yapılmıştır. Çalışma, olasılıksal sismik tehlike analizi ile tsunami sayısal modellemesini ilişkilendirmektedir. Monte Carlo simülasyon tekniği kullanılarak 100 adet deprem içeren sentetik deprem kataloğu oluşturulmuştur. Bu katalog, fay mekanizmasinin oluşturabileceği en yüksek deprem büyüklüğü aralığı olarak hesaplanan Moment büyüklük 6.5 ve 7.1 arasında olan depremleri içermektedir ve katolog içerisinde her olay için oluşma olasılıkları ve bağlı tsunami dalga yükseklikleri hesaplanmıştır. Tsunami sayısal simulasyonlari doğrusal olmayan sığ su denklemleri kullanan NAMI DANCE tsunami sayısal kodu ile gerçekleştirilmiştir. Tsunami sayısal modelleme sonuçlarına göre, farklı zaman ölçekleri için, en düşük ve en yüksek su yüzeyi seviyesi ve yüksekliği ve karadaki en yüksek akım derinliği ile ilgili olasılık dağılımı sunulmaktadır. Ayrıca, akım derinliğinin 0.3 m'yi aşma olasılığı ile ilişkili baskın haritaları ve sentetik ölçüm noktalarında 0.3 m tsunami dalga yüksekliğinin aşılma olasılıkları gösterilmiştir. Çalışma sonucunda Tuzla bölgesinde 1 m'ye varan tsunami dalga yüksekliklerinin 50 yıllık tekrarlanma süresinde %65 aşma olasılığına sahip olduğu ve önümüzdeki 100 yıl içinde oluşma olasılıklarının %85'e ulaştığı elde edildi. Aynı zamanda su baskın alanındaki akım derinlikleri 50 ve 100 yıl içinde sırasıyla %60 ve %80 olasılıkları ile 1 m'yi geçtiği hesaplanmıştır. Önümüzdeki 500 ve 1000 yıla baktığımızda ise, depremlerin meydana gelme olasılıklarının çok yüksek olduğu gözükmektedir. Su baskın haritaları sonuçları, 50 ve 100 yıllık maruz kalma süreleri için, 0.3 m olarak kabul edilen eşik akım derinliği

değerinin aşılma olasılığının %10 ile %75 arasında değiştiğini göstermektedir. Çalışma alanında su baskın mesafesi en yüksek 60 m olarak hesaplanmıştır. Sentetik ölçüm noktalarında ise, dalga yüksekliği eşik değeri 0.3 olarak kabul edildiğinde, noktalardan yalnızca birkaç tanesi %75 - %85 arasında bir oluşma olasılığına sahiptir ve bu olasılık değeri 100 yıllık maruz kalma süresi için %90' a kadar çıkar. 500 ve 1000 yıllık süre içinde deprem oluşma olasılıkları,karakteristik depremlerin oluşma periyotlarının bu süre içinde kalması sebebiyle %95'ten fazla olarak hesaplanmıştır.

TABLE OF CONTENTS

ACKNOWLEDGEMENTS iii
ABSTRACT iv
ÖZET vi
LIST OF FIGURES ix
LIST OF TABLES xii
LIST OF TABLES xii
LIST OF SYMBOLS xiii
LIST OF ACRONYMS/ABBREVIATIONS xiv
1. INTRODUCTION 1
2. LITERATURE SURVEY 3
2.1. An Overview of Previous Researches on Tectonism in the Marmara Sea 3
2.2. Previous Studies on Probabilistic Hazard Analyses in the Marmara Sea & Information on Monte Carlo Simulation Technique 6
3. METHODOLOGY 12
3.1. Study Area 12
3.2. PTHA Method using Monte Carlo Simulation Technique 15
3.3. Determination of Earthquake Magnitude Range 16
3.4. Determination of Hypocenter 17
3.5. Probability Calculations 18
3.6. Tsunami Numerical Modelling 21
4. RESULTS AND DISCUSSION 29
4.1. Graphs of Probability of Occurrences for the Entire Synthetic Earthquake Catalogue 29
4.2. Tsunami Inundation Maps in Tuzla Test Site 37
4.3. Synthetic Gauge Points 46
4.4. Uncertainties in PTHA and Monte Carlo Simulations 48
5. CONCLUSION 50
6. FURTHER STUDIES 53
REFERENCES 54

LIST OF FIGURES

Figure 2.1. General tectonic map of the study area. The westward movement of the Anatolian block results from (1) differences in rates of motion between the Arabian and African plates, (2) different directions of motion between the Anatolian block and Eurasian plate to the north, and (3) subduction of the African plate beneath the Anatolian block at the Hellenic and Florence trenches. The Arabian plate is moving to the north faster than the African plate, both relative to a stable Eurasian plate. The result is a westward moving wedge incorporating most of Turkey (USGS, 2000 [1] ; modified from Barka (1992) [2] and Rockwell, 2001 [3]). 4

Figure 2.2. Bathymetric map of the North Marmara Fault System (Modified from Armijo et al., 2002 [4]). 5

Figure 2.3. Maximum inundation depths resulting from the probabilistic simulations for 10% probability of exceedance in 50 years ([5]). . . . 8

Figure 3.1. Tuzla Test Site and the Location of Prince Islands Fault Segment 13

Figure 3.2. Some Important Locations at Tuzla Domain 14

Figure 3.3. Probability Density Function for BPT Model According to Different Earthquake Magnitudes and Recurrence Times. 20

Figure 3.4. Nested Domains 26

Figure 3.5. Tuzla Study Domain with Coastline and Buildings 27

Figure 4.1. Probabilities of Exceedance Corresponding to Maximum Water Surface Elevation, Minimum Water Surface Elevation and Flow Depth on Land for the next 50 years. 31

Figure 4.2. Probabilities of Exceedance Corresponding to Maximum Water Surface Elevation, Minimum Water Surface Elevation and Flow Depth on Land for the next 100 years. 33

Figure 4.3. Probabilities of Exceedance Corresponding to Maximum Water Surface Elevation, Minimum Water Surface Elevation and Flow Depth on Land for the next 500 years. 35

Figure 4.4. Probabilities of Exceedance Corresponding to Maximum Water Surface Elevation, Minimum Water Surface Elevation and Flow Depth on Land for the next 1000 years. 36

Figure 4.5. Probabilistic Tsunami Inundation Maps for Tuzla Study Domain representing the Probability of Exceedance of 0.3 m Inundation Depth within the Next 50 and 100 Years. 39

Figure 4.6. Probabilistic Tsunami Inundation Maps of Northern Part of Tuzla Study Domain representing the Probability of Exceedance of 0.3 m Inundation Depth for the Next 50 and 100 Years. 41

Figure 4.7. Probabilistic Tsunami Inundation Maps for the Southern Part of Tuzla Study Domain representing the Probability of Exceedance of 0.3 m Inundation Depth for the Next 50 and 100 Years. 43

Figure 4.8. Probabilistic Tsunami Inundation Maps of Shipyard Area in Tuzla Study Domain representing the Probability of Exceedance of 0.3 m Inundation Depth for the Next 50 and 100 Years. 45

Figure 4.9. Probability of Exceedance of 0.3 m Tsunami Wave Height within the next 50, 100, 500 and 1000 years at Synthetic Gauge Points. . 47

LIST OF TABLES

Table 3.1. Table of Fault Parameters 15

Table 3.2. Maximum Positive and Negative Initial Tsunami Wave Amplitudes, Magnitude, Depth and Displacement For Each Earthquake Scenario 22

Table 3.3. Matrix Sizes of Four Nested Domains 27

Table 3.4. Run time of NAMI DANCE according to time passes after the earthquake rupture (simulation time). 28

LIST OF SYMBOLS

a	Coefficient
A	Fault Area
b	Standard Error
D	Slip of a Fault (m)
L	Fault Length
Mo	Seismic Moment
$\dot{M}o$	Moment Rate
M_w	Moment Magnitude
t	Elapsed Time from the Last Characteristic Event (yr)
ΔT	Condition that a characteristic earthquake occurs in the next ΔT years.
Tr	Earthquake Recurrence Time (yr)
V	Long Term Slip Rate on a Fault (mm/yr)
W	Fault Width
α	Aperiodicity
μ	Shear Modulus

LIST OF ACRONYMS/ABBREVIATIONS

BPT	Brownian Passage Time
GIS	Geographic Information Systems
MC	Monte Carlo
NAF	North Anatolian Fault
NAFZ	North Anatolian Fault Zone
NSW	Nonlinear Shallow Water
PIF	Prince Islands Fault
PSHA	Probabilistic Seismic Hazard Analysis
PTHA	Probabilistic Tsunami Hazard Analysis

1. INTRODUCTION

Marmara Region, especially highly populated coastal cities along the coasts of the Marmara Sea, is the heart of Turkish economy in terms of having great number of industrial facilities in largest capacity and potential, refineries, ports and harbors. Recent studies and evaluation of earthquake recurrence periods revealed that there is a high possibility of having an earthquake with magnitude up to Mw 7.0 in Prince Islands fault. According to Ambraseys, (2002) [6], the latest earthquake happened on this fault system in 1766 and until that time the fault has been accumulating the energy. Recent studies show that, the probability of occurrence of M>7 earthquake beneath the Marmara Sea is 35-70% in the next 16 years [7]. The megacity Istanbul is also located in Marmara Sea and the area is one of the most seismically active areas in Turkey. The North Anatolian Fault Zone controls the great part of the seismic activity in the Marmara Sea region. Due to these circumstances, Istanbul with a population of more than 14 million is under the threat of high damage due to this possible big earthquake and also triggered tsunamis.

In previous studies, tsunami analyses were mostly performed in deterministic manner using various earthquake scenarios depending on the combinations of different fault parameters without considering probability of occurrences. However, in this study tsunami hazard assessment is done for Tuzla region in the light of high possibility of occurrence of a big earthquake in Marmara Sea. Probabilistic tsunami hazard analysis (PTHA) is performed for selected test site Tuzla, as one of the most important points along the coast of the Marmara Sea, in relation to the probability of earthquake occurrences in Prince Islands fault.

Probabilistic tsunami hazard assessment is important, because it takes into account all possible earthquakes in a fault even they occur with very low probability and when decision makers design coastal zones and structures, especially critical ones, they would consider the results of probabilistic studies. There have been various deterministic tsunami hazard assessment studies done around the world. Within the scope

of these studies, tsunami scenario database and worst-case inundation maps prepared for the coastal zones. However, the results of the deterministic studies are sometimes rather overestimated for coastal structures. For instance, if deterministic tsunami analyses results are of the 2011 Great East Japan Tsunami are taken into consideration for the design of coastal defence structures along east Japan coasts, very huge seawalls should be constructed for tsunami prevention. In that case, people in these coastal regions should live behind such giant walls which would not be acceptable for most of them even one can claim it as for the sake of this people. Therefore, as recent strategy of tsunami hazard mitigation, regional and local authorities tend to know the possibility of the occurrence of such tsunami events s in the region in order to decide the most appropriate ways for tsunami prevention instead of forcing people to live behind such huge walls for a disaster with 1000-year return period.

In this thesis, literature survey, that have been done in order to better understand the tectonic evolution, fault mechanisms and historical events of Marmara Region, and probabilistic tsunami hazard assessment application for some places around the world, are explained in Chapter 2. Besides, in the same chapter some previous studies on probabilistic tsunami hazard analysis in the Marmara Sea are presented together with the reference information regarding Monte Carlo Simulation Technique. In Chapter 3, methodology of probabilistic tsunami hazard analysis, Monte Carlo simulation technique, probability calculations, tsunami numerical modelling and determination of some earthquake parameters are described in detail. In Chapter 4, the results of this study are discussed and finally conclusions and suggestions for further studies are given in Chapter 5.

2. LITERATURE SURVEY

As mentioned in previous sections, Prince Islands Fault (PIF) is selected for PTHA in Tuzla test site. In order to perform reliable tsunami hazard analyses, tectonism as well as seismic activity in PIF should be better understood for the whole Marmara Sea. For this purpose, a detailed literature survey has been conducted including both seismic and probabilistic studies in this region. Section 2.1 gives the literature survey for seismic studies while Section 2.2 presents probabilistic hazard studies previously performed in Marmara Sea, that become as basic references of PTHA in this study.

2.1. An Overview of Previous Researches on Tectonism in the Marmara Sea

In the Marmara Sea, the biggest part of the tectonism is controlled by the North Anatolian Fault Zone. NAFZ is one of the biggest strike-slip plate boundaries in the world. The fault starts from the Karlıova triple junction in the east and extends about 1200 km to Northern Aegean ([2] , [8] , [9]). It sets apart the Anatolia and Eurasia due to the northward migration of Arabian Plate in the east and southward rollback of the Hellenic subduction zone in the west ([10] , [11] , [12]). Earthquakes along the NAF especially has right-lateral strike-slip faulting mechanism. However, normal faulting earthquakes are observed in the western part of the fault because of the transtensional setting of Aegean Sea region ([11], [13]).

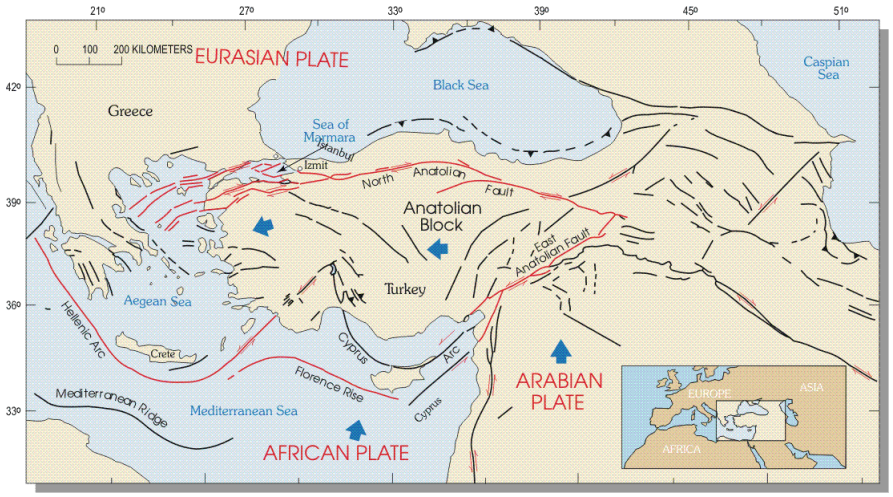


Figure 2.1. General tectonic map of the study area. The westward movement of the Anatolian block results from (1) differences in rates of motion between the Arabian and African plates, (2) different directions of motion between the Anatolian block and Eurasian plate to the north, and (3) subduction of the African plate beneath the Anatolian block at the Hellenic and Florence trenches. The Arabian plate is moving to the north faster than the African plate, both relative to a stable Eurasian plate. The result is a westward moving wedge incorporating most of Turkey (USGS, 2000 [1] ; modified from Barka (1992) [2] and Rockwell, 2001 [3]).

The Marmara Sea region is a transition zone between the strike-slip regime of the NAF and the extension regime of the Aegean Sea area. The northern branch of the NAFZ forms a major transtensional NW–SE right bend under the Sea of Marmara at Çınarcık trough ([14]). The fault trace is attached to the complex Central Marmara and Tekirdağ pull-apart basins, before join the NE-SW striking Ganos fault on land by following the northern margin of the Marmara Sea. Finally, the fault exits into the Aegean Sea by way of Saros Gulf ([15], [16], [4], [17], [18], [19], [14]. The fault trace beneath the Marmara Sea is not directly observable. Therefore, making a segmentation model for the offshore parts of the NAFZ is difficult ([20], [21], [17], [4], [22], [23]).

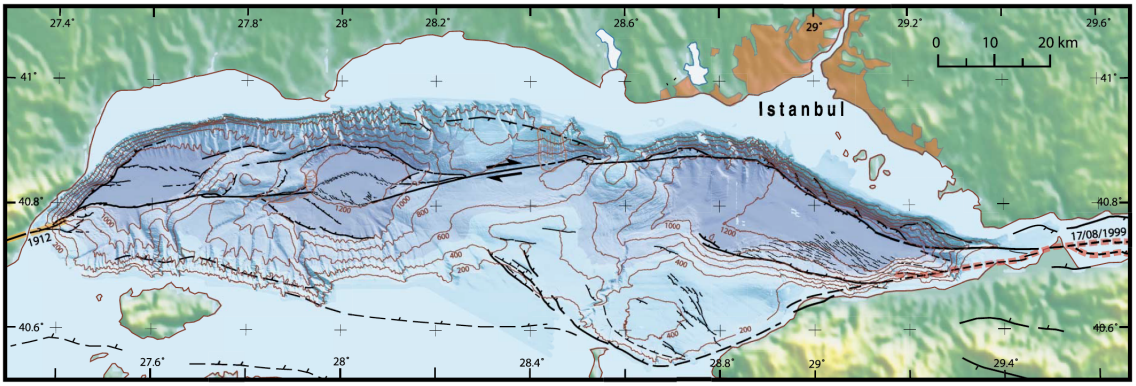


Figure 2.2. Bathymetric map of the North Marmara Fault System (Modified from Armijo et al., 2002 [4]).

The current right-lateral slip rate along the NAFZ is $\sim$ 25 mm/yr ([24], [25]).The eastern and the central part of the fault have relatively simple structure with almost pure strike-slip motion formed on a single fault trace ([26]). In the western side, the motion between the Anatolia and Eurasia plates is accommodated across the Marmara region by $\sim$ 19 mm/yr of right-lateral slip and 8 mm/yr of extension ([27], [11]). Slip rates of the main Marmara fault ranging between 17-28 mm/yr ([28], [25]). On the other hand, Hergert and Heidbach (2010) [29] suggests that the right-lateral slip rate on the main Marmara fault is between 12.8-17.8 mm/yr because of slip partitioning and internal deformation. The Prince Islands fault (PIF) segment is actively accumulating strain since 1766 event. The rate-lateral slip rate for the PIF and Çınarcık basin is 15$\pm$2 mm/yr and in addition to this, the fault has 6$\pm$2 mm/yr of extension ([30]) and in this study, 17mm/yr is used for average long term slip rate on the fault.

Bohnhoff et al. (2013) [31] also emphasize that 150 km long part of NAFZ along the Marmara Sea has been silent since 22 May 1766 earthquake although NAF has experienced two M>7 earthquakes in August 1912 Ganos and August 1999 Izmit earthquakes recently. Before 1766 event, an earthquake in 1754 September happened in eastern parts of the Sea of Marmara and it ruptured the 36 km lenght of PIF ([6]).

The historical documents reveal that the region has been experienced many earthquake-related tsunamis in the past. According to Altinok et al. (2011) [32],

35 tsunami events happened in Marmara Sea between BC 330 and 1999. For instance, 1894 earthquake was triggered a tsunami and the sea inundated 200 m in Istanbul ([33], [34]). The recent one happened after the 17 August 199 Izmit earthquake and several small faults and submarine failures generated 10 m high tsunami waves at the southern shore of the Izmit gulf.

In Marmara Sea, arrival time of tsunami waves is also very short. As earthquakes are expected in Marmara Sea with the rupture of segments of North Anatolian Fault (NAF) in near future, the region should be investigated in terms of the possibility of tsunamis by the occurrence of earthquakes in specific return periods.

2.2. Previous Studies on Probabilistic Hazard Analyses in the Marmara Sea & Information on Monte Carlo Simulation Technique

Probabilistic tsunami hazard analysis (PTHA) aims to examine the probability of a specific tsunami hazard parameter, such as maximum tsunami wave height or inundation height, exceedance within a certain return periods at a specific location. The results of the analysis are generally expressed as a hazard curve. These curves demonstrate the exceedance level of the hazard parameter as a function of probability. This method allows reduce the effect of tsunami hazard in coastal regions ([35]).

PTHA have been applied in various scales, local, regional and global to give an information to different policy decisions ([35]). In the global scale, PTHA have been undertaken to prioritize resources for Disaster Risk Management by estimating multi-hazard risk which used by the United Nations Office for Disaster Risk Reduction ([36], [37], [38]). Moreover, various regional scale, such as Pacific Ocean, Mediterranean Sea etc., PTHA studies have been done to determine the high hazard locations and the tsunami sources ([35]).

The steps to be followed in PTHA can be listed as (i) definition of potential tsunami sources and mechanisms, calculation of annual recurrence rate, (ii) numerical modelling of the generation and propagation of tsunami waves, (iii) the probability

calculation of exceeding a certain wave amplitude for a given period of time and at a specific location ([39]).

The first step of the PTHA is derived from Probabilistic Seismic Hazard Analysis (PSHA) ([40]). Numerical modelling of tsunami waves are combined with the probability of the source because, historical tsunami catalogues are not sufficient to make quantitative predictions on probability calculation of exceedance a certain wave amplitude ([35]). PSHA can be separated as time-dependent and time-independent models ([41]). The time-independent model depends on the acceptance of the probability of an earthquake occurrence fits a Poisson distribution. The mean recurrence time is the only required parameter for calculation of time-independent probability and results do not change in time. Time dependent model, on the other hand, probability of an earthquake depends on the elapsed time which is the time since the last event and the model fits a renewal mode, Brownian passage time (BPT) or any other distribution. This model requires recurrence time of earthquake, variability of the frequency of events and elapsed time ([42]).

As the second step of the PTHA, numerical modelling of tsunami waves gives principal tsunami hydrodynamic parameters throughout the study area. These parameters are the important part of the tsunami risk assessment ([43]), they allow to estimate damage to the structures, economic impact and fatalities and this gives an important information about setting priorities for the expenditure of financial and human resources on risk mitigation efforts ([44], [38], [45], [46], [47], [48]).

There has been a wide range of studies in Marmara Sea region regarding the fault mechanisms, seismic activities, earthquakes and triggered tsunamis. The region is attractive because of its complex structure and high possibility of an earthquake occurrence with the magnitude of larger than 7.0 offshore Istanbul mega-city. The recent studies reveal that the probability of occurrence of such an earthquake beneath the Marmara Sea is 35 - 70% within the next 16 years ([7]). As investigating the probability of a tsunami which can be generated by an earthquake with known probability of occurrence become popular among researchers very recently, quite few number of

researches on PTHA in the Marmara Sea is available.

One of the example for those researches is Hancilar (2012) [5] which prepared inundation maps based on probabilistic and deterministic tsunami hazard analyses for Istanbul. In the study, first of all tsunamigenic seismic sources were identified in the Marmara Sea region. 26 tsunamigenic zones were determined with their fault mechanisms, thickness and geographical locations. After the seismic zonation, probabilistic and deterministic tsunami hazard assessment and inundation mapping was performed for Istanbul. The results of the study show that maximum inundation distance at the south of the Küçükçekmece Lake is about 600 m and this value is also remarkable in the coast of Kadıköy and from Kartal to Tuzla for a 10% probability of exceedance in 50 years. Additionally, deterministic part of the analyses argues that the area between the Marmara Sea and Küçükçekmece Lake and Kartal-Pendik-Tuzla coast are the most risky regions that exposed to tsunami heights possibly greater than 3 m ([49], [50]).

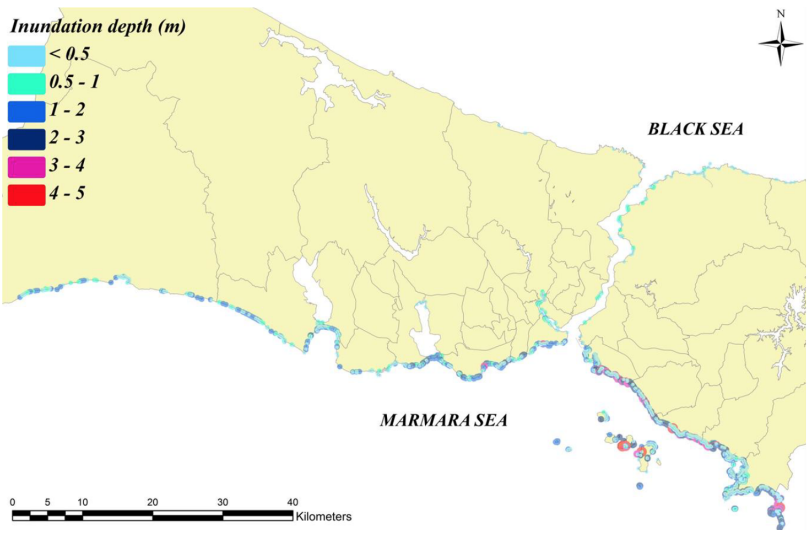


Figure 2.3. Maximum inundation depths resulting from the probabilistic simulations for 10% probability of exceedance in 50 years ([5]).

Another probabilistic tsunami study in Marmara Sea is Murru et al. (2016) [14] in which time-dependent and time-independent earthquake ruptures in the Marmara Sea region are estimated for the next 30 years. In this study, a fault segmentation model is identified by associating with seismological data and slip rates of each segment. They

used several probability models to show recurrence time probability distribution. In the time-dependent Brownian passage time (BPT) probability model the probability density function was calculated based on expected recurrence time, the elapsed time from the last characteristic event and aperiodicity of the distribution ([51]). They found that Poisson probability of an earthquake with M>7.3 is 35% and when time dependence and stress transfer are considered this probability increases to 47% for the next 30 years.

Looking at the probabilistic seismic hazard analyses (PSHA) in Marmara region, one of the most significant study is Erdik et al. (2004) [52] which aimed to develop seismic hazard maps for Marmara region. In this study, they separate faults into 25 segments both in sea and land. They consider not only independent segment rupture but also rupture of several fault segments by cascading methodology. The results are predicted by Poisson distribution and the time-dependent model and results show that time-dependent analysis results 1.1 to 1.3 times the Poisson analysis for Istanbul region.

Kankan et al. (2009) [53] also performed probabilistic seismic hazard analysis in Marmara region. They used smoothed-gridded seismicity model and fault model as two different earthquake source models. For the first model earthquake catalog with magnitude between M 4 and 6.5, for the fault model earthquakes with magnitude larger than m 6.5 are used. Moreover, they used Poisson model (time-independent) for probability calculations. According to their results, average 0.4 g PGA is expected with 10% probability of exceedance in the next 50 years in Istanbul.

In this study, probabilistic tsunami hazard analysis (PTHA), as becoming recently a widely used procedure for coastal zones, is performed for Tuzla region. In tsunami research, this method has been applied for various tsunami source, such as earthquakes, landslide, volcanic activity etc. For the earthquake generated tsunamis, the method generally adapted from seismic hazard assessment methods [54]. For regional studies, hazard curves can be generated by empirical analysis using available tsunami runup data. However, if such data is not available, Monte Carlo simulation, a computational based method widely used in PSHA, should be considered as a primarily method to

generate tsunami hazard curves [40].

Monte Carlo simulation technique is generally applied to generate earthquake catalogue of a given length of time. In this technique, a list of earthquakes is generated using the frequency–magnitude relationship for each seismic source [55]. Seismic zonation should be done by considering regions that have relatively homogeneous earthquake activity and faulting regimes [56]. After that, tsunami numerical modelling is performed for each event of this synthetic catalogue and tsunami hydrodynamic parameters, mainly maximum wave heights flow depths, current velocities, as well as tsunami inundation zones are estimated. Regional PTHA studies can be used as a guide for further local studies to develop of a more effective tsunami warning systems. Tsunami risk assessment will serve the best for the needs of societies when associate regional studies with the local ones [56]. In this study, totally the same way of Monte Carlo simulation techniques is followed in analyses.

To sum up tsunami and seismic hazard analyses in the Marmara Sea with probabilistic approach, Hancilar (2012) have made a probabilistic tsunami hazard assessment based on 26 tsunamigenic fault zones and prepared inundation maps along the coast of Istanbul. On the other hand, Murru et al. (2016) have calculated earthquake probabilities on the faults by using both time-dependent and time-independent models. Moreover, Erdik et al. (2004) have generated seismic hazard maps for Marmara region using both Poisson and time-dependent model. Finally, Kankan et al. (2009) have performed probabilistic seismic hazard analyses for Marmara reigon. In the light of the previous studies described above in detail and with the enthusiasm of having new PTHA approach in Marmara Sea, probabilistic tsunami hazard maps are prepared for Tuzla test site using the methodology followed in this study is given in Chapter 4.

Referring to the previous researches in Marmara Sea in regard to fault models and seismicity, time-dependent probability model and tsunami numerical modelling studies are developed accordingly. This study depends on the fully characteristic fault model and considers the probability of one specific fault's rupture, that is Prince Islands Fault (PIF). As stated in Bohnhoff et al. (2013) [31], the rupturing of PIF is known

as having specific return period and this fault has not generated an earthquake since 1754. This means that the fault has been accumulating significant seismic energy and the probability of occurrence of its rupture is increasing year by year. This fault also has a potential to generate a tsunami after an earthquake. Therefore, PTHA is aimed to make in Marmara Sea mainly focusing on test site Tuzla for the preparation of high resolution tsunami inundation maps and distribution of hydrodynamic parameters due to the probability of occurrence of associated earthquakes in PIF determined by Monte Carlo Simulations. Having the country's biggest shipyard and many other important facilities and being vulnerable against tsunami damage due to proximity to PIF, the region should be investigated in terms of tsunami hazard in probabilistic way. The details of selection of Tuzla test site and PTHA methodology are given in Chapter 3.

3. METHODOLOGY

3.1. Study Area

Istanbul is one of the most important of the seven cities along the coast of the Marmara Sea. It is literally the heart of Turkey's economy as hosting many industrial facilities, global large-scale companies with a population of more than 14 million. Besides Istanbul has significant importance in terms of economic, historical and socio-cultural heritage.

Tuzla is one of the coastal district of Istanbul and located on the southernmost part of the city (Figure 3.1). The region includes several residential area but the most critical point about the region is that Tuzla has the biggest shipyard area not only in the Marmara Sea but also in Turkey (Figure 3.2). The region is about 20 km away from the PIF and this situation increases the potential of the earthquake and tsunami damage for this area.

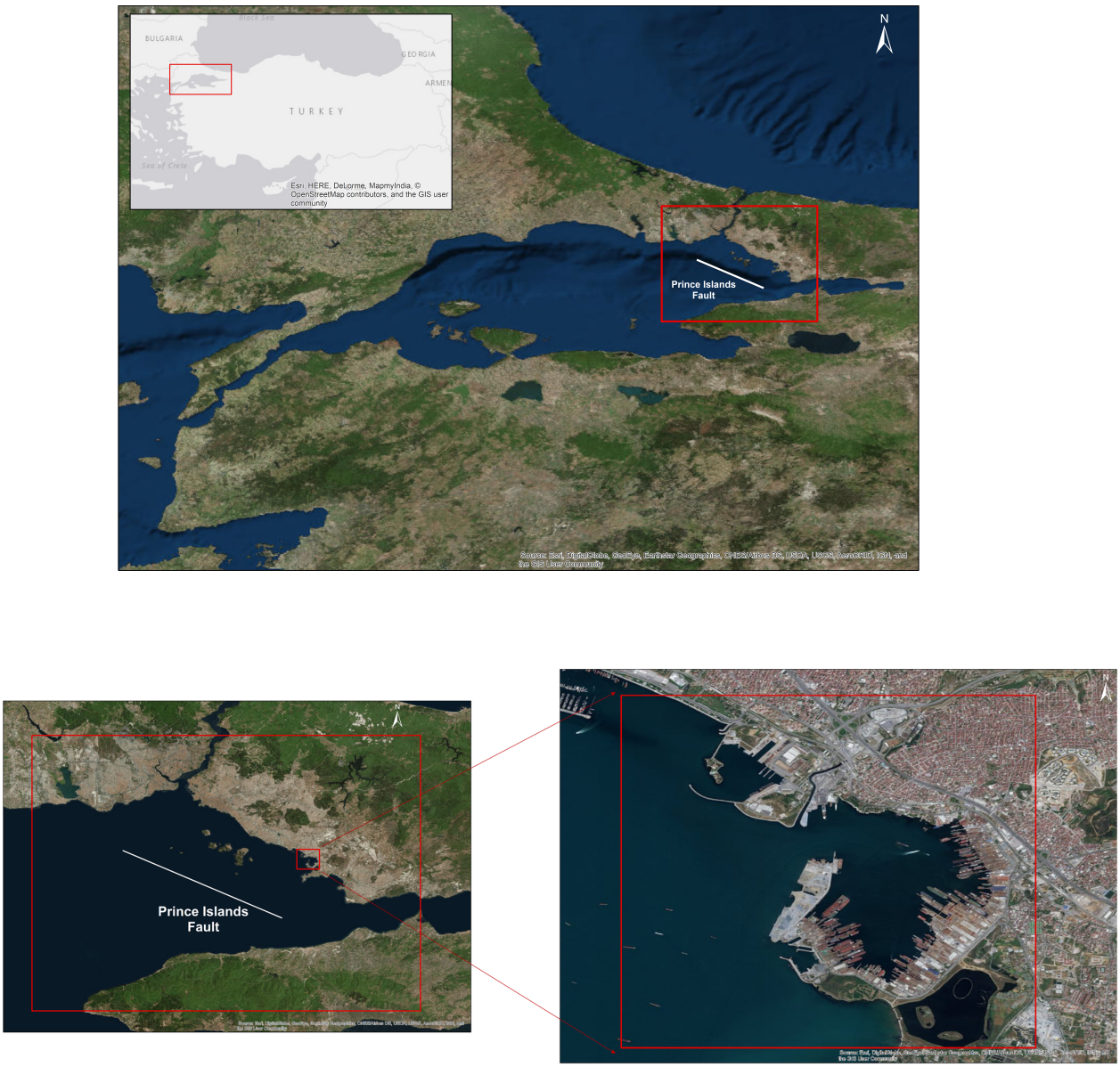


Figure 3.1. Tuzla Test Site and the Location of Prince Islands Fault Segment



Figure 3.2. Some Important Locations at Tuzla Domain

3.2. PTHA Method using Monte Carlo Simulation Technique

In this study, a synthetic earthquake catalogue is generated using Monte Carlo simulation technique because historical catalogue for Prince Islands fault segment is not sufficient to make the probabilistic hazard analysis using different probabilistic methods such as Gutenberg-Richter law or the Kernel method.

As described in literature survey, PIF is fully characteristic and a characteristic earthquake will rupture entire fault and release the whole energy. Therefore, while performing Monte Carlo simulations, area of the fault and fault parameters (strike, dip and rake angles) are used as constant referring to the outcomes of EU 7th Frame Project MARSITE ([57]). Table 3.1 gives the fault parameters used as constant in this study.

Table 3.1. Table of Fault Parameters

Fault Length (km)	Fault Width (km)	Strike	Dip	Rake
33.5	14	119	80	210

A MatLab code is prepared for MC simulations which selects the earthquake magnitude and depth randomly depending on the specified reliable ranges. The ranges for magnitude and depth of characteristic earthquakes are selected according to literature survey and related equations which will be described in following section.

Monte Carlo simulation technique allows to generate a list of earthquakes based on a frequency-magnitude relationship. This technique depends on a uniformly distributed source model and it provides equal chance to each source. As a result, synthetic earthquake catalogue will have uniformly random distributed earthquake sources ([55]). To sum up, Monte Carlo simulation method generates random numbers based on a specified distribution ([58]).

Using Monte Carlo simulation, a synthetic earthquake catalogue is generated by selecting magnitude and depth randomly and using area and directivity of the fault

as a constant (3.1). Monte Carlo simulations were performed 100 times to get 100 different earthquake scenarios.

According to Monte Carlo-based synthetic earthquake catalogue, initial tsunami wave heights (tsunami source) are calculated using Okada (1985) [59] equations. In this study, 100 earthquake scenarios are used as a tsunami source and tsunami numerical modelling is performed for each tsunami source.

3.3. Determination of Earthquake Magnitude Range

Earthquake magnitude and displacement on the fault surface are one of the parameters randomly selected by the Monte Carlo technique. Therefore, it is necessary to define a range for earthquake magnitude and calculate the displacements for each earthquake magnitude.

Based on a characteristic earthquake model, individual faults tend to rupture entire fault when a large earthquake happened. This model accepts that characteristic earthquake releases all of the seismic energy and the magnitude of the earthquake depends on the dimension of the fault ([60]).

In this case, only the Prince Islands fault, with approximately 34 km length and 14 km width, is considered as an earthquake source ([57], [61]). This fault zone is assumed that it has a potential to generate a characteristic earthquake and according to Wells and Coppersmith (1994) [62] scaling relation between fault area and magnitude (3.1), this fault can generate a characteristic earthquake with the magnitude varies between Mw 6.5-7.1.

$$Mw = a + b * log(L * W) \tag{3.1}$$

In this equation, a and b are coefficient and standard errors, L is fault length and W is the fault width.

Displacement calculation for each magnitudes are done using the formulation of Aki (1966) [63],

$$D = \frac{Mo}{\mu \dot{A}} = \frac{10^{(Mw+6.07)*1.5}}{\mu A} \tag{3.2}$$

where D is displacement on the fault surface, Mw is moment magnitude, μ is the shear modulus, and A is the fault area.

3.4. Determination of Hypocenter

Seismogenic thickness and the location of the earthquake is another important parameter required for earthquake and tsunami source. At first, the Prince Islands fault zone is accepted as fully characteristic and an earthquake should rupture the entire fault area. Therefore, it is assumed that if the rupture starts at the center of the fault and continues in two directions, the fault will rupture entirely. For this reason, the locations of the earthquakes is accepted as middle point of the Prince Islands fault zone ([57]).

For the seismogenic thickness, the study of the Karabulut et al. (2003) [64] shows that the seismic activity of the northern segment of NAF starts at the depth of 5 km. The bottom of the seismogenic thickness can be determined based on another study which shows the after-shock activity of the 17 August 1999 İzmit Earthquake ([61]). The results of the study indicate that the earthquakes in the Tuzla cluster, that is located on the northern scarp of the Çınarcık basin, are observed between the depths of 5 and 14 km. The mechanism of events between the depth of 5 and 10 km shows normal faulting. On the other hand, strike-slip mechanism dominates the depths below

10 km to 14 km. As a result, seismic activity can be observed between the depths of 5-14 km and fault plane solutions show normal and strike-slip mechanisms in this area.

3.5. Probability Calculations

In this study, probabilistic tsunami hazard analyses are performed for Tuzla region in the case of the Prince Islands Fault rupture. Historical records show that, this fault generates an earthquake with the recurrence interval of about 250 years and the latest event occurred in 1766 ([6]). However, this event caused to rupture of the 58 km long northern part of NAF from Izmit to Tekirdağ ([65], [66]). According to Ambraseys and Jackson (2000) [66], the event that happened on 2 September 1754 is the latest characteristic event for the Prince Islands segment and it caused the rupture of a 36 km long fault segment. In the scope of these information, time dependent probabilistic model is used in the study.

In the time-dependent approach, the Prince Islands Fault is considered as a fully characteristic with the recurrence time T_r. The mean recurrence interval of earthquakes (T_r) can be defined as the ratio between the mean moment of repeat earthquakes (seismic moment) and the long-term moment accumulation rate on the fault (moment rate). Seismic moment can be obtained using the formulation of Kanamori (2004) [67] and the moment rate of the fault is calculated from fault area and long-term slip rate of the fault ([68]).

$$T_r = \frac{Mo}{\dot{M}o} = \frac{10^{(Mw+6.07)*1.5}}{\mu V A} \tag{3.3}$$

In this equation, Mw is moment magnitude, μ is the shear modulus, V is long term slip rate in mm/yr and A is the fault area. The moment magnitude value in the equation 3.3 was selected randomly using Monte Carlo simulations. Thus, seismic moment (Mo) and the mean recurrence time (T_r) were calculated for each earthquake

scenario.

Long term slip rate is also selected as 17 mm/yr based on the literature survey for the equation 3.3 ([30]).

For the probability calculation, time-dependent Brownian passage time (BPT) probability model is used to obtain the recurrence time probability of the earthquake in the fault segment. The probability density function for BPT model ([51]) is given by

$$f(t, T_r, \alpha) = (\frac{T_r}{2\pi\alpha^2 t^3})^{1/2} exp[\frac{(t - T_r)^{1/2}}{2T_r\alpha^2 t}] \tag{3.4}$$

where t is the elapsed time from the last characteristic event and α is the aperiodicity (also known as the coefficient of variation). This parameter defines the regularity of the expected characteristic earthquakes on the fault and varies between the 0.3 and 0.7. In this study, aperiodicity, which is known as the parameter defines the how expected characteristic earthquake occurs regularly or irregularly on any fault segment ([14]), was taken as 0.5 ([7]).

In BPT model, the function starts at zero rapidly after the last characteristic event and it rises with elapsed time (t) closing to the recurrence time (T_r). Figure 3.5 clearly shows that trend for different earthquake magnitudes. The recurrence time of the earthquakes with small magnitudes is about 30 years. Because of that, the function increasing rapidly and it shows a big probability density within a short time period. On the other hand, the recurrence time of big earthquakes is extremely big with respect to small ones. These earthquakes have small probabilities and they need long time periods to generate an earthquake.

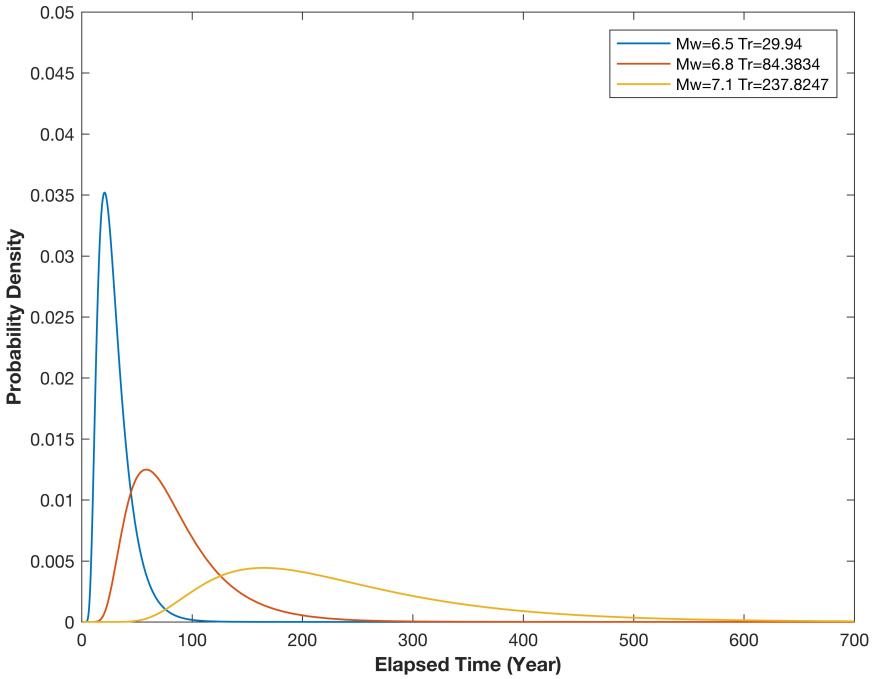


Figure 3.3. Probability Density Function for BPT Model According to Different Earthquake Magnitudes and Recurrence Times.

Probability of the earthquake occurrence on the fault is calculated based on the probability density function. The basic concept of the probability is that the area under the density function gives the probability of the earthquake. Therefore, probability of the earthquakes can be calculated using the following equation:

$$P(t, \Delta T) = \frac{\int_t^{t+\Delta T} f(t)dt}{\int_t^{t+\infty} f(t)dt} \tag{3.5}$$

where ΔT is the condition that a characteristic earthquake occurs in the next ΔT years. In this case, probability of a characteristic earthquake was calculated using ΔT as 50, 100, 500 and 1000 years.

In the next chapter, tsunami simulations will be described in details. The probability of exceedance of a selected wave height, flow depth (inundation depth) and

inundation distance will be associated with the probability of occurrence of that earthquake since tsunami modelling is directly based on the parameters of earthquakes and their probability of occurrence can be assigned as the probability of exceedance of those those tsunami parameters.

3.6. Tsunami Numerical Modelling

Tsunami simulations are performed for each earthquake in synthetic catalogue using tsunami numerical model NAMI DANCE (NAMI DANCE, 2011) which was developed by researchers Andrey Zaytsev, Ahmet Cevdet Yalciner, Bora Yalciner, Anton Chernov, Efim Pelinovsky and Andrey Kurkin. NAMI DANCE is the user-friendly version of TUNAMI-N2 ([69]) developed in C++ language which computes all fundamental parameters of tsunami motion in shallow water and in the inundation zone using explicit numerical solution of shallow water wave equations with finite-difference technique and allows for better understanding of the effect of the tsunami waves ([70], [71]). NAMI DANCE can solve both Linear and Nonlinear Shallow Water (NSW) Equations with selected coordinate system (Cartesian or spherical) and calculates the tsunami motion. NSW equations is preferable in deep water because of reasonable computer time and memory and also calculates the results in acceptable error limit ([72]). The NAMI DANCE is validated and verified using NOAA standards and criteria for tsunami currents and inundation ([73], [74]). The numerical solutions are tested, validated and verified against analytical solutions, laboratory measurements and field observations ([75] [76], [77]).

NAMI DANCE calculates tsunami generation using Okada (1985) equations. In this study, water surface distribution of tsunami source (initial wave amplitude) are calculated with this method for 100 earthquakes in the synthetic earthquake catalogue prepared as a result of MC simulations. Table 3.2 shows the maximum positive and negative wave amplitudes calculated by Okada (1985) equations for each earthquake scenario.

Table 3.2: Maximum Positive and Negative Initial Tsunami Wave Amplitudes, Magnitude, Depth and Displacement For Each Earthquake Scenario

ID	Magnitude (Mw)	Depth (km)	Displacement on the Fault Surface (m)	Max. Negative Amplitude (m)	Max. Positive Amplitude (m)
EQ-1	6.7	12.904	1.0156	-0.0881	0.0486
EQ-2	7	5.1436	2.8622	-0.4516	0.2623
EQ-3	6.8	8.6621	1.4345	-0.1692	0.0958
EQ-4	6.6	11.574	0.71896	-0.0684	0.038
EQ-5	7	10.112	2.8622	-0.3027	0.1697
EQ-6	6.9	5.6254	2.0263	-0.3064	0.1773
EQ-7	6.7	9.429	1.0156	-0.113	0.0636
EQ-8	6.9	13.423	2.0263	-0.1696	0.0934
EQ-9	6.8	8.068	1.4345	-0.1772	0.1007
EQ-10	6.5	9.9575	0.50899	-0.0544	0.0306
EQ-11	6.9	12.675	2.0263	-0.1785	0.0987
EQ-12	6.7	7.0229	1.0156	-0.1364	0.0781
EQ-13	6.7	9.2186	1.0156	-0.1148	0.0647
EQ-14	6.9	13.209	2.0263	-0.1721	0.0949
EQ-15	6.7	5.8959	1.0156	-0.15	0.0866
EQ-16	6.6	6.1866	0.71896	-0.1036	0.0597
EQ-17	7.1	13.493	4.043	-0.3368	0.1854
EQ-18	6.6	8.2395	0.71896	-0.0876	0.0497
EQ-19	6.7	5.9966	1.0156	-0.1487	0.0858
EQ-20	6.5	10.87	0.50899	-0.0509	0.0284
EQ-21	7.1	7.9995	4.043	-0.5022	0.2855
EQ-22	6.7	9.9099	1.0156	-0.109	0.0612
EQ-23	7.1	9.9781	4.043	-0.4318	0.2423

EQ-24	6.8	13.847	1.4345	-0.1167	0.0641
EQ-25	6.8	6.2472	1.4345	-0.2056	0.1184
EQ-26	6.6	5.5596	0.71896	-0.1093	0.0633
EQ-27	6.6	9.691	0.71896	-0.0784	0.0441
EQ-28	6.8	8.8715	1.4345	-0.1665	0.0941
EQ-29	6.6	5.0648	0.71896	-0.1143	0.0664
EQ-30	7.1	10.363	4.043	-0.4197	0.235
EQ-31	6.7	12.021	1.0156	-0.0936	0.0519
EQ-32	7.1	6.2015	4.043	-0.5817	0.335
EQ-33	7	7.7988	2.8622	-0.3612	0.2056
EQ-34	6.7	12.457	1.0156	-0.0908	0.0503
EQ-35	6.5	13.919	0.50899	-0.0412	0.0226
EQ-36	6.7	12.478	1.0156	-0.0907	0.0502
EQ-37	6.7	12.143	1.0156	-0.0928	0.0515
EQ-38	6.6	5.8854	0.71896	-0.1063	0.0614
EQ-39	7.1	7.6177	4.043	-0.5177	0.2951
EQ-40	6.6	12.813	0.71896	-0.0627	0.0346
EQ-41	6.6	10.173	0.71896	-0.0757	0.0424
EQ-42	6.8	8.047	1.4345	-0.1775	0.1009
EQ-43	6.8	11.099	1.4345	-0.1412	0.0787
EQ-44	6.5	8.6231	0.50899	-0.0602	0.0341
EQ-45	6.7	12.104	1.0156	-0.0931	0.0516
EQ-46	6.9	12.293	2.0263	-0.1833	0.1015
EQ-47	7.1	12.125	4.043	-0.37	0.2051
EQ-48	6.8	7.5799	1.4345	-0.1842	0.105
EQ-49	6.9	11.726	2.0263	-0.1907	0.106
EQ-50	6.5	11.57	0.50899	-0.0484	0.0269
EQ-51	6.6	9.6642	0.71896	-0.0786	0.0442
EQ-52	7	12.014	2.8622	-0.264	0.1464
EQ-53	6.5	10.808	0.50899	-0.0512	0.0286

EQ-54	6.5	8.2604	0.50899	-0.0619	0.0352
EQ-55	6.8	7.2522	1.4345	-0.1892	0.1081
EQ-56	6.7	9.5682	1.0156	-0.1118	0.0629
EQ-57	6.6	8.4435	0.71896	-0.0863	0.0489
EQ-58	7	11.125	2.8622	-0.2812	0.1567
EQ-59	6.9	11.278	2.0263	-0.1969	0.1097
EQ-60	6.7	12.724	1.0156	-0.0892	0.0493
EQ-61	6.7	6.4009	1.0156	-0.1437	0.0826
EQ-62	6.6	11.407	0.71896	-0.0692	0.0385
EQ-63	6.6	5.8205	0.71896	-0.1069	0.0617
EQ-64	7	12.981	2.8622	-0.2469	0.1362
EQ-65	7.1	8.4753	4.043	-0.4839	0.2742
EQ-66	7	11.445	2.8622	-0.2748	0.1529
EQ-67	6.6	9.4268	0.71896	-0.08	0.0451
EQ-68	6.9	9.1501	2.0263	-0.2303	0.1299
EQ-69	6.6	13.531	0.71896	-0.0597	0.0329
EQ-70	6.6	10.066	0.71896	-0.0763	0.0428
EQ-71	6.9	12.031	2.0263	-0.1867	0.1035
EQ-72	7	5.7349	2.8622	-0.4286	0.2478
EQ-73	7	7.7769	2.8622	-0.3618	0.206
EQ-74	7	12.957	2.8622	-0.2473	0.1365
EQ-75	6.6	10.763	0.71896	-0.0725	0.0405
EQ-76	6.7	11.245	1.0156	-0.0989	0.0551
EQ-77	6.8	11.28	1.4345	-0.1394	0.0776
EQ-78	7.1	8.947	4.043	-0.4666	0.2636
EQ-79	6.6	6.8351	0.71896	-0.0981	0.0562
EQ-80	6.8	9.7705	1.4345	-0.1556	0.0874
EQ-81	6.9	6.8795	2.0263	-0.2755	0.1579
EQ-82	6.7	10.231	1.0156	-0.1065	0.0597
EQ-83	6.6	7.3442	0.71896	-0.0941	0.0537

EQ-84	6.7	10.782	1.0156	-0.1023	0.0571
EQ-85	6.7	5.4516	1.0156	-0.1559	0.0903
EQ-86	6.6	7.2487	0.71896	-0.0948	0.0542
EQ-87	7	13.824	2.8622	-0.2332	0.1281
EQ-88	6.8	7.2035	1.4345	-0.1899	0.1086
EQ-89	6.9	5.7938	2.0263	-0.3019	0.1744
EQ-90	6.6	10.87	0.71896	-0.0719	0.0402
EQ-91	6.8	13.358	1.4345	-0.1206	0.0664
EQ-92	6.5	6.3042	0.50899	-0.0726	0.0418
EQ-93	6.8	13.151	1.4345	-0.1223	0.0674
EQ-94	6.7	9.0539	1.0156	-0.1163	0.0656
EQ-95	6.9	5.7603	2.0263	-0.3028	0.175
EQ-96	6.9	9.3019	2.0263	-0.2276	0.1283
EQ-97	6.7	13.532	1.0156	-0.0844	0.0464
EQ-98	6.8	10.032	1.4345	-0.1526	0.0856
EQ-99	6.9	7.7793	2.0263	-0.2561	0.1458
EQ-100	6.9	11.648	2.0263	-0.1918	0.1066

In this study, tsunami hydrodynamic parameters are calculated both in Marmara Sea and Tuzla region. The main parameters focused in this study are the tsunami wave heights and flow depths on land and the results will be shown in the terms of probability of exceedance of a given wave height and flow depth within the next 50, 100, 500 and 1000 years.

Before starting tsunami simulations, the necessary inputs should be prepared precisely in order to obtain reliable results. Bathymetry data is one of the most important input in NAMI DANCE that significantly effects the reliability of results especially in shallow water zone due to the nature of NSW Equations. Therefore, the bathymetry data in the smallest domain includes digitized coastline, ports and buildings in high resolution.

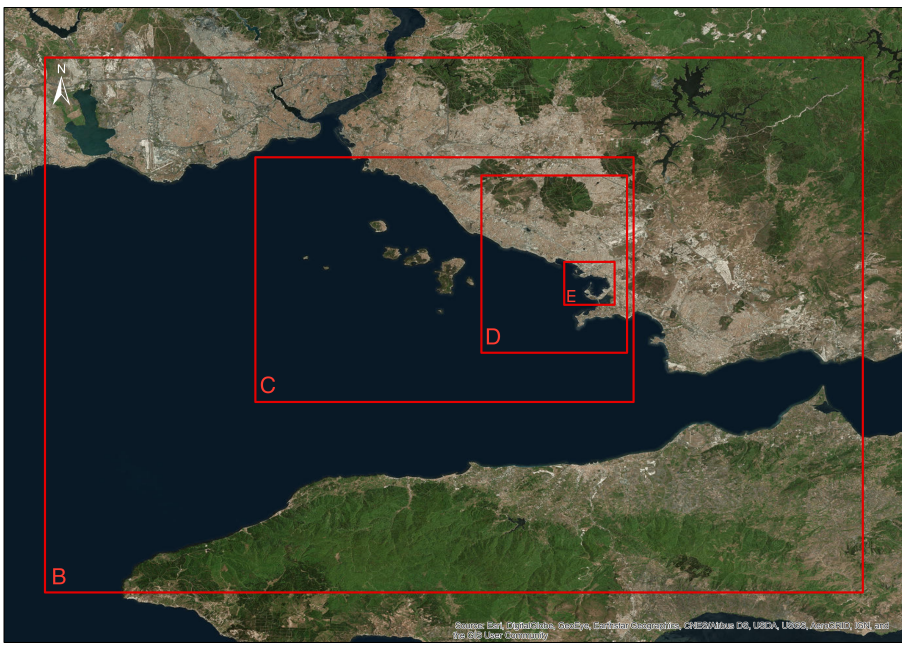


Figure 3.4. Nested Domains

NAMI DANCE can make nested analyses under the condition that grid size of study domains have a certain ratio. Therefore, four nested domains are generated, with the coarsest grid size as 81 m and the finest grid size as 3 m, in GIS environment. In Figure 3.4, the boundaries of these four nested domains are represented. The smallest domain focuses on the Tuzla region and as emphasized before, the bathymetry data

includes detailed features in high resolution. In Figure 3.5, Tuzla study domain with building and coastline can be seen. Matrix sizes (number of columns and rows) of these four nested domains can be seen in Table 3.3.



Figure 3.5. Tuzla Study Domain with Coastline and Buildings

Table 3.3. Matrix Sizes of Four Nested Domains

Domain	Grid Size (m)	Matrix Size
Domain-B	81	891 x 584
Domain-C	27	1334 x 863
Domain-D	9	1422 x 1737
Domain-E	3	2126 x 1804

NAMI DANCE was recently developed in GPU environment which significantly decreases the run time and therefore enables to perform huge amount of simulations in large matrix sizes of study domains within extremely short time. As an example of the performance of NAMI DANCE GPU version, Table 3.4 shows the run time of the program in order to make analyses with four nested domains corresponding to time passed after earthquake occurs.

Table 3.4. Run time of NAMI DANCE according to time passes after the earthquake rupture (simulation time).

Time passed after earthquake origin time	Run Time of NAMI DANCE GPU version (min.)
30 Min.	7.2
1 Hour	14.5
2 Hours	30

Synthetic gauge point file is another required input of the NAMI DANCE. In addition to calculation of principal tsunami hydrodynamic parameters, program can also calculate water level and current velocity changes over time in every gauge points. Therefore, various gauge points are selected along the coast of nested domains, near shore and off shore and close to some important buildings on land.

During the inundation of tsunami waves, current velocity is an important tsunami parameter in land and sea, especially in ports and basins. This parameter may cause dragging and landing of sea vessels inside the port. Basic tsunami parameters such as tsunami wave amplitude, flow depth and current velocity, can be calculated by NAMI DANCE. In this study, the results are represented based on the probability of exceedance of given threshold for water surface elevation and flow depth.

4. RESULTS AND DISCUSSION

In this chapter, the results of the PTHA for Tuzla test site are represented in the terms of three different visualization categories for 50, 100, 500 and 1000 years exposure time. First, graphics are prepared to show general distribution of probability of occurrence with respect to minimum and maximum water surface elevation and maximum flow depth on land. Second, tsunami inundation maps that show probability of exceedance of 0.3 m inundation depth for different exposure time, are generated for Tuzla region in order to observe flooded areas and their probabilities clearly. And finally, the probability map of exceedance of 0.3 m wave heights at synthetic gauge points are represented as bar charts.

4.1. Graphs of Probability of Occurrences for the Entire Synthetic Earthquake Catalogue

The graphics are generated to demonstrate the probabilities of occurrences corresponding to the minimum and maximum water surface elevations and maximum flow depths on land calculated from tsunami sources of each earthquake in synthetic earthquake catalogue using MatLab.

It should be noted that in case of having same magnitude of earthquakes in two different earthquake scenario of the catalogue, the probability of occurrences of these scenarios would be the same. However, since they would have different seismic depths the tsunami initial wave height calculated by Okada (1985) will be different which results the calculation of different hydrodynamic parameters. As a result, the graphs show different maximum water surface elevations having the same probability of occurrences.

The graphics show that there is more than one value of tsunami hydrodynamic parameter are calculated for the same probability value.In order to obtain a best-fitted single representative curve, MatLab Custom Equation fitting method was applied to

each graphics. The non-linear least-squares fitting process is used in this method and it selects optimal default starting points of coefficients randomly selected between 0 and 1. The procedure also allows to calculate confidence bounds for the fitted coefficients.

Graphics also include 95% of confidence bounds for fitted coefficients, residuals plot and goodness of fit statistics. According to these graphics, the probability of exceedance of a specific wave height and inundation depth for different time scales can be predicted. There is an inverse proportion between probability and tsunami hydrodynamic parameters as earthquakes with lower probability of occurrence have a potential to generate larger tsunami waves when time increases.

In Figure 4.1, graphics of probabilities of occurrences according to maximum and minimum water surface elevation (maximum withdrawing) and inundation depth for next 50 years are represented, respectively. According to these graphs, tsunami waves up to 1 m and withdrawal of the waves near to -1 m have approximately 65% probability of occurrence. Tuzla region includes various shipyards, ports and any other important facilities. Therefore, probability of the withdrawal of the water is important as much as probability of maximum water surface elevation. 1 m height of wave withdrawal may cause the ships to be stranded at the ports and results extreme financial losses. The probability for 1 m inundation depth, on the other hand, can be predicted as about 60%. Residuals of the graphics varies between the 0.2 and -0.2.

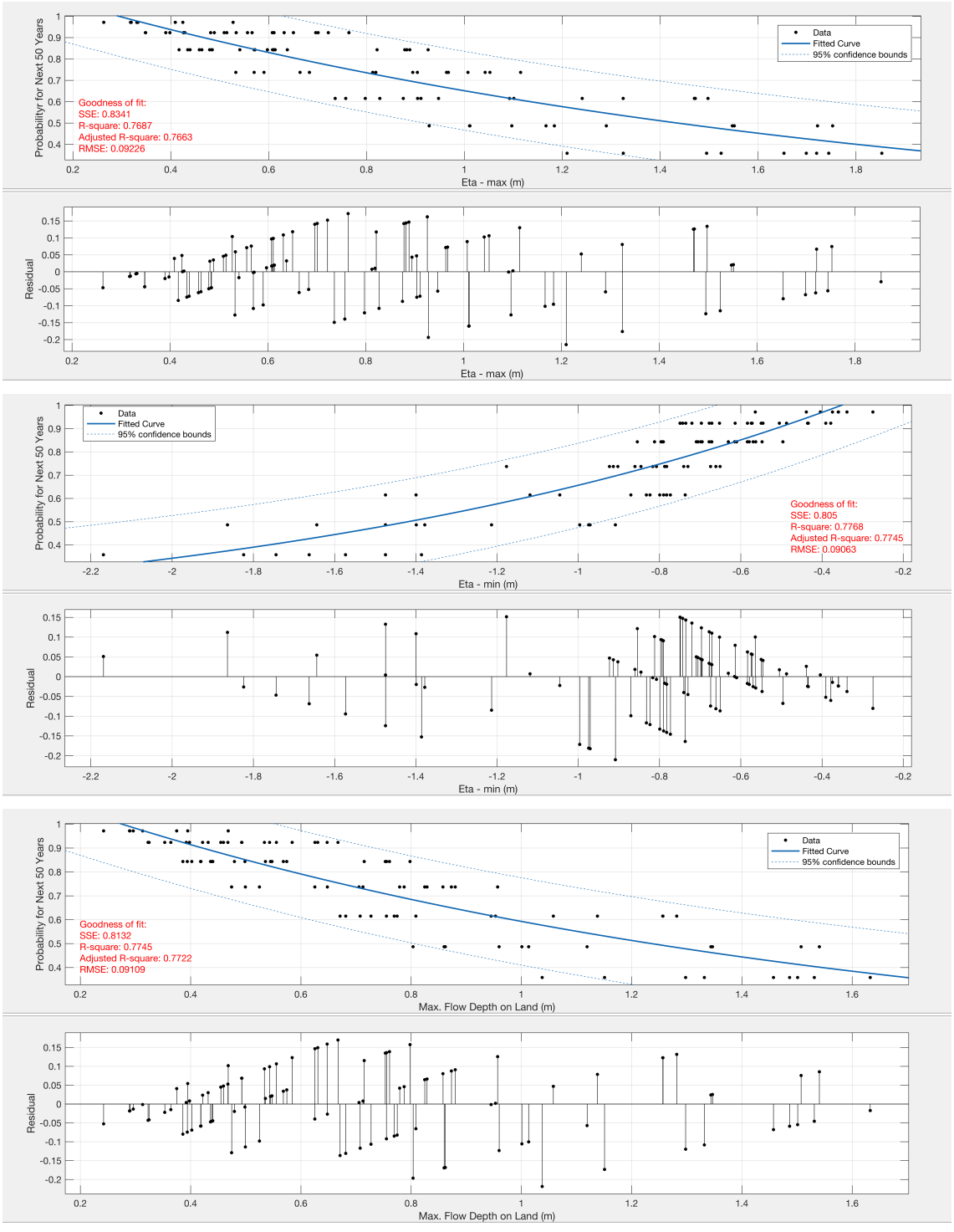


Figure 4.1. Probabilities of Exceedance Corresponding to Maximum Water Surface Elevation, Minimum Water Surface Elevation and Flow Depth on Land for the next 50 years.

The situation for 100-year exposure time (Figure 4.2) clearly shows that probabilities of occurrences increase with the time. The probability of exceedance of 1 m water surface elevation and 1 m wave withdraw reaches up to 85%. Probability of exceedance of inundation depth also changes dramatically. The probability of exceedance of 1 m inundation depth is found around 80% from the graphics. Residuals also reduces and changes between the 0.1 and -0.2.

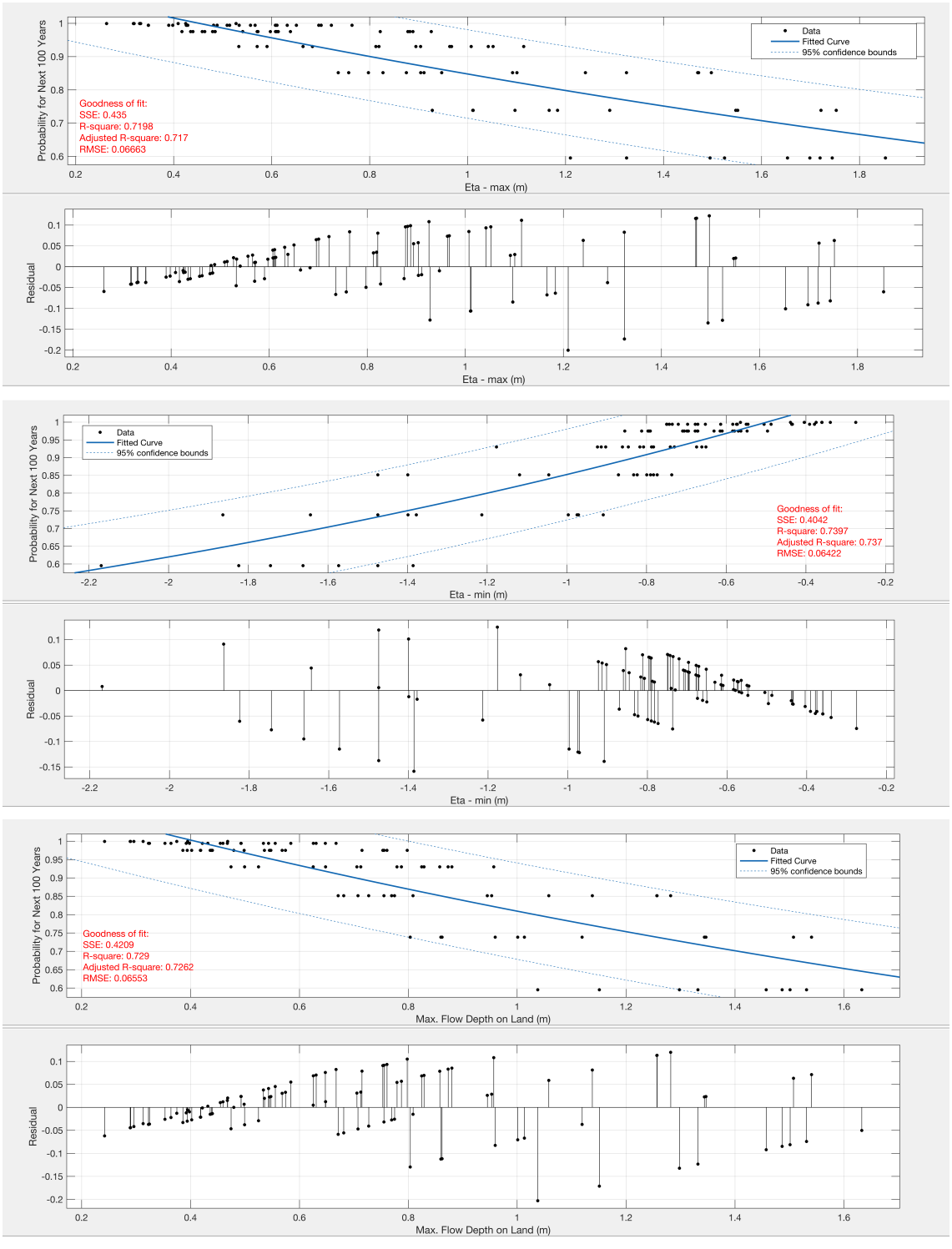


Figure 4.2. Probabilities of Exceedance Corresponding to Maximum Water Surface Elevation, Minimum Water Surface Elevation and Flow Depth on Land for the next 100 years.

Figure 4.3 and 4.4 demonstrate that probabilities are very high and they are very close to 100% probability of occurrence for next 500 and 1000 years. Besides, residuals approach to zero. This occurs due to short return period of earthquake rupture of PIF, mentioned as around 250 years ([31]).

Considering the results of the whole simulations, maximum water surface elevation, minimum water surface elevation (maximum withdrawing) and inundation depth are calculated in worst case earthquake scenario as 1.85 m, -2.16 m and 4.4812 m respectively. The probabilities of occurrence of these values are 35% for next 50 years, 60% for next 100 years and 99% for the next 500 and 1000 years.

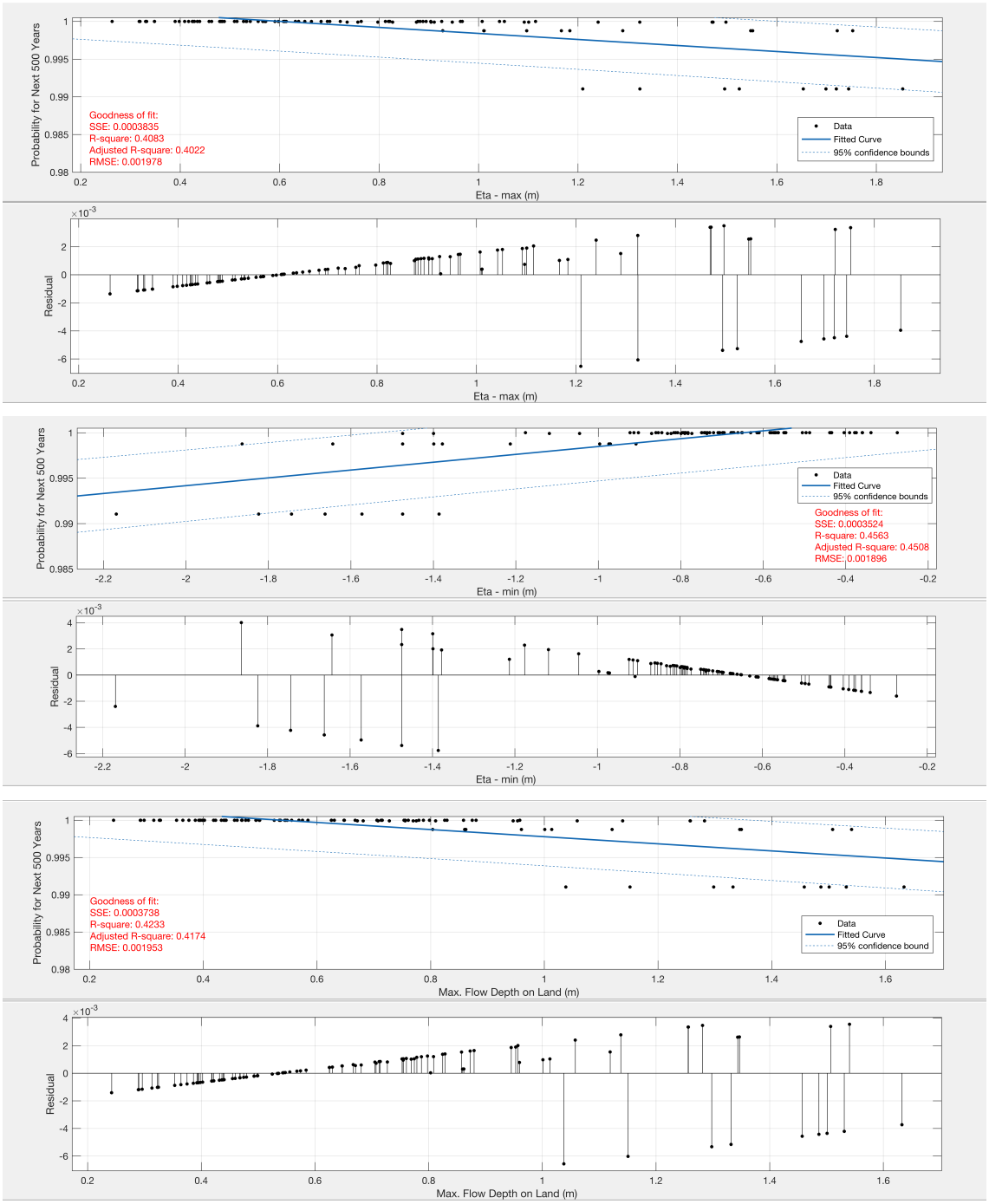


Figure 4.3. Probabilities of Exceedance Corresponding to Maximum Water Surface Elevation, Minimum Water Surface Elevation and Flow Depth on Land for the next 500 years.

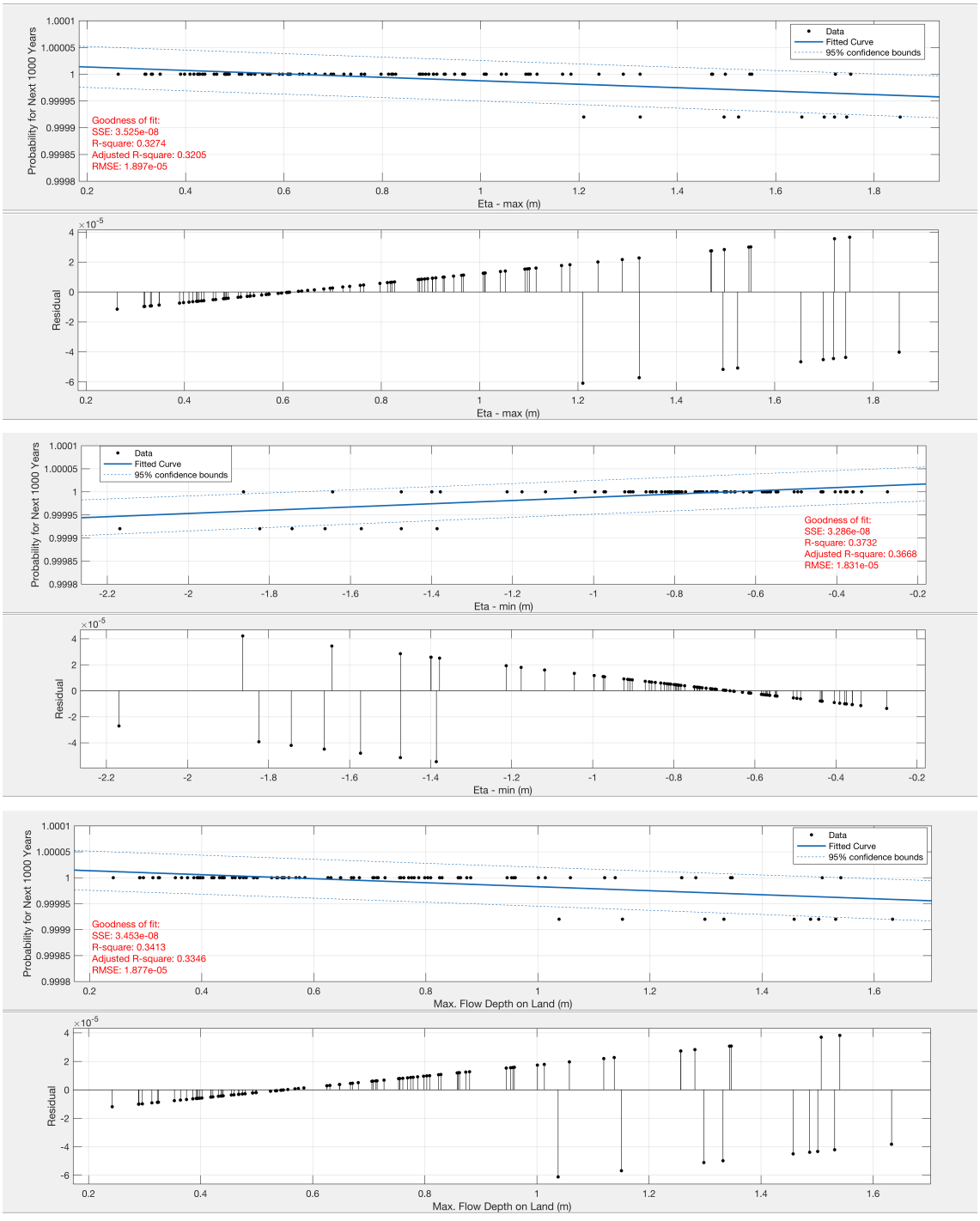


Figure 4.4. Probabilities of Exceedance Corresponding to Maximum Water Surface Elevation, Minimum Water Surface Elevation and Flow Depth on Land for the next 1000 years.

4.2. Tsunami Inundation Maps in Tuzla Test Site

Inundation maps of Tuzla domain are also generated for 50 and 100 years exposure time in GIS environment. Even if flow depth is a few centimeters, it can lead to serious coastal damage due to the high power of the waves. Therefore, these inundation maps have a great significance to understand the flooded areas in study domain and the amount of penetrated water. Designers and decisions makers can make their plan referring to these inundation maps.

Generation of inundation maps are based on the probability of exceedance of 0.3 m flow depth. Tsunami waves with 0.3 m height have a potential to fall a person and for this reason this value was selected as the threshold ([78], [79]). For this reason, only the earthquake scenarios, that generated inundation depths larger than or equal to 0.3 m, are considered. The flow depth values calculated as spatial distribution of maximum flow depths at each grid node are replaced with the probability of occurrence of the respective earthquake scenario. This procedure is repeated for the whole 100 scenarios. After that, the mean (average) flow depth values are calculated at each grid node and thus the spatial distribution of probability of exceedance of 0.3 m flow depth in inundation zone is obtained (Figure 4.5). Red zones in inundation maps correspond to the flow depth with highest probability. The change of colors from red to green represents the decreasing of probability of exceedance and therefore the flow depth, at the same time. Inundation maps also show that some parts of the region are more likely to inundate because of low ground elevation. These places should be protected from tsunami waves by filling and increasing the ground elevation.

Flow depth files, which is one of the output of the NAMI DANCE, are taken for each scenario and changed the flow depth value with its probability. After that, the mean (average) of these files are calculated and thus probability of exceedance 0.3 m flow depth could be mapped on average of whole scenarios. Red zones, in maps, correspond to flow depth with highest probability.The change of colors from red to green represents the decreasing of the water depth and the occurrence probability, at the same time. Inundation maps are also show that some parts of the region are more

likely to inundate because of low elevation. These places should be protected from tsunami waves by filling and increasing the elevation.

Figure 4.5 shows the inundation maps of study domain for 50 and 100-year exposure time. Most of the area in Tuzla shipyard region have probability of exceedance between 10% and 20% for both exposure time of 50 and 100 years. However, some places in the northern and southern part of the area and inside the bay show larger than 75% probability of inundation within the next 100 years. Maximum inundation distance is observed as around 60 m in the test site.

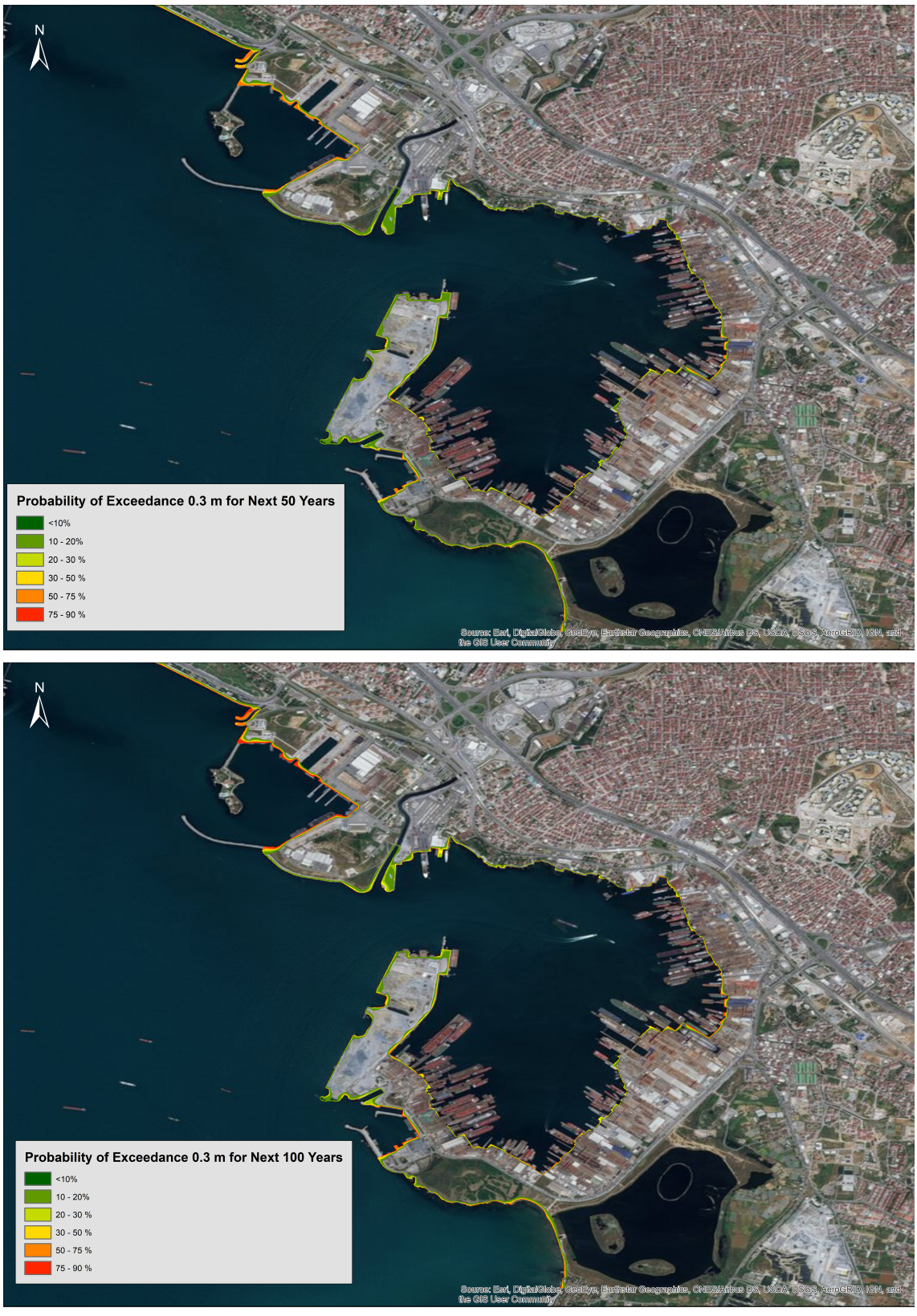


Figure 4.5. Probabilistic Tsunami Inundation Maps for Tuzla Study Domain representing the Probability of Exceedance of 0.3 m Inundation Depth within the Next 50 and 100 Years.

In Figure 4.6, probabilistic inundation maps of one of the most important locations in study region are represented for the next 50 and 100 years. This area has a significance because it is a shipyard belonging to Turkish Naval Forces and military ships are built and repaired in this area. The area has high potential to expose tsunami waves with probability larger than 50% for the next 50 years exposure time. In 100 years, this probability increases and varies between 75% and 90%. No significant inundation zone is observed along the coast of the seawall and the peninsula. This may be due to the high ground elevation of these zones. Tsunami waves are inundated up to 45 m inside the small bay. This inundation distance could cause severe damage to shipyard and other constructions if corresponding current velocities are also significant.

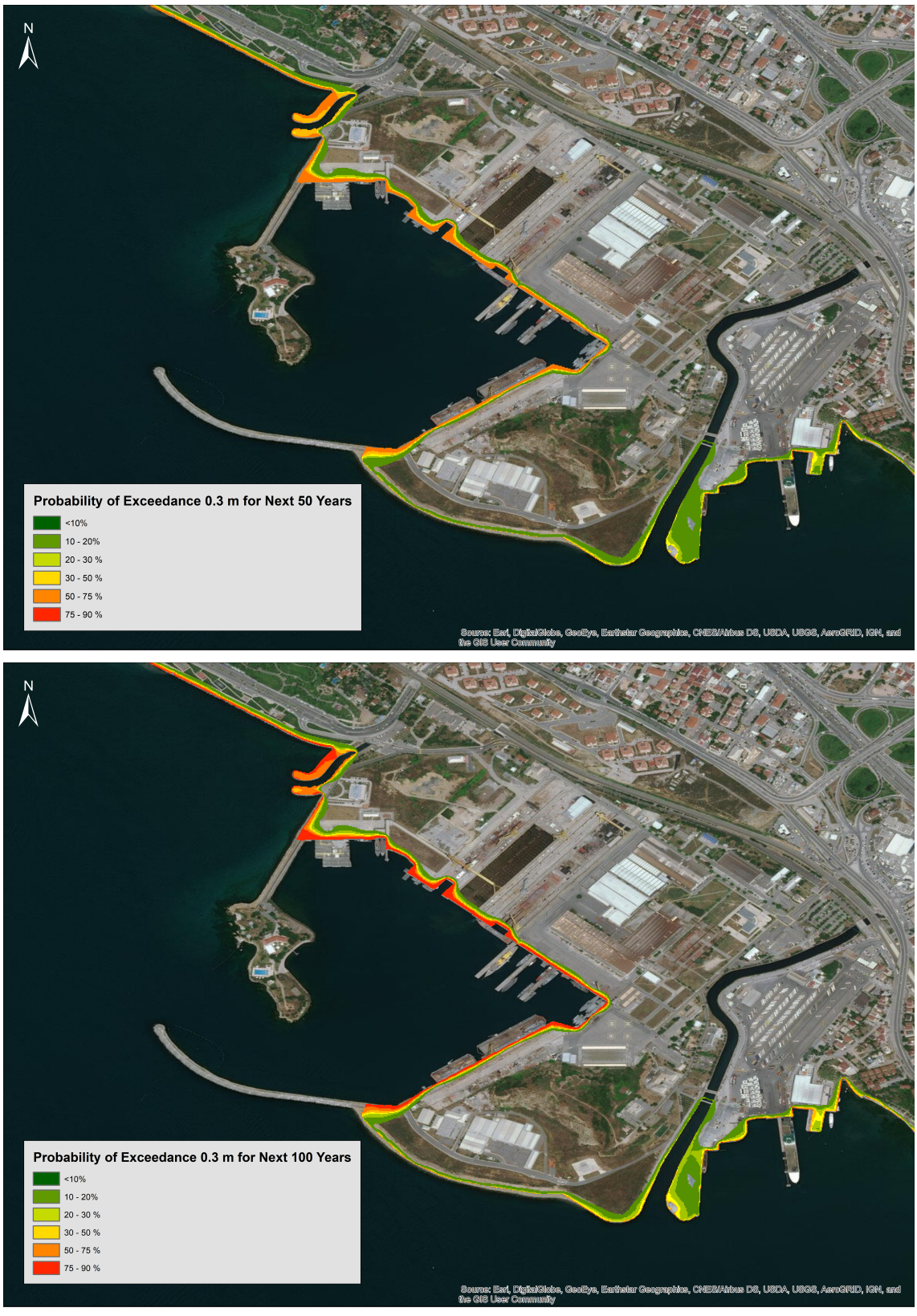


Figure 4.6. Probabilistic Tsunami Inundation Maps of Northern Part of Tuzla Study Domain representing the Probability of Exceedance of 0.3 m Inundation Depth for the Next 50 and 100 Years.

In the next figure (4.7), the southern part of the Tuzla study area can be seen according to probabilities of inundation for the next 50 and 100 years. Very limited area in the coastal zone is inundated with the probability between 30% and 50% within the next 50 years. The probability reduces up to 10% some inner locations from the coastline. For 100 years exposure time, the situation is almost the same. Only minor parts of the region, at the south, approaches to 75% - 90% probability of exceedance of 0.3 m inundation depth threshold. The maximum inundation distance is calculated about 60 m. This does not include any important structure and the effect of the tsunami will be minimal. The inundation distance decreases up to 10 m at the other parts of the region.

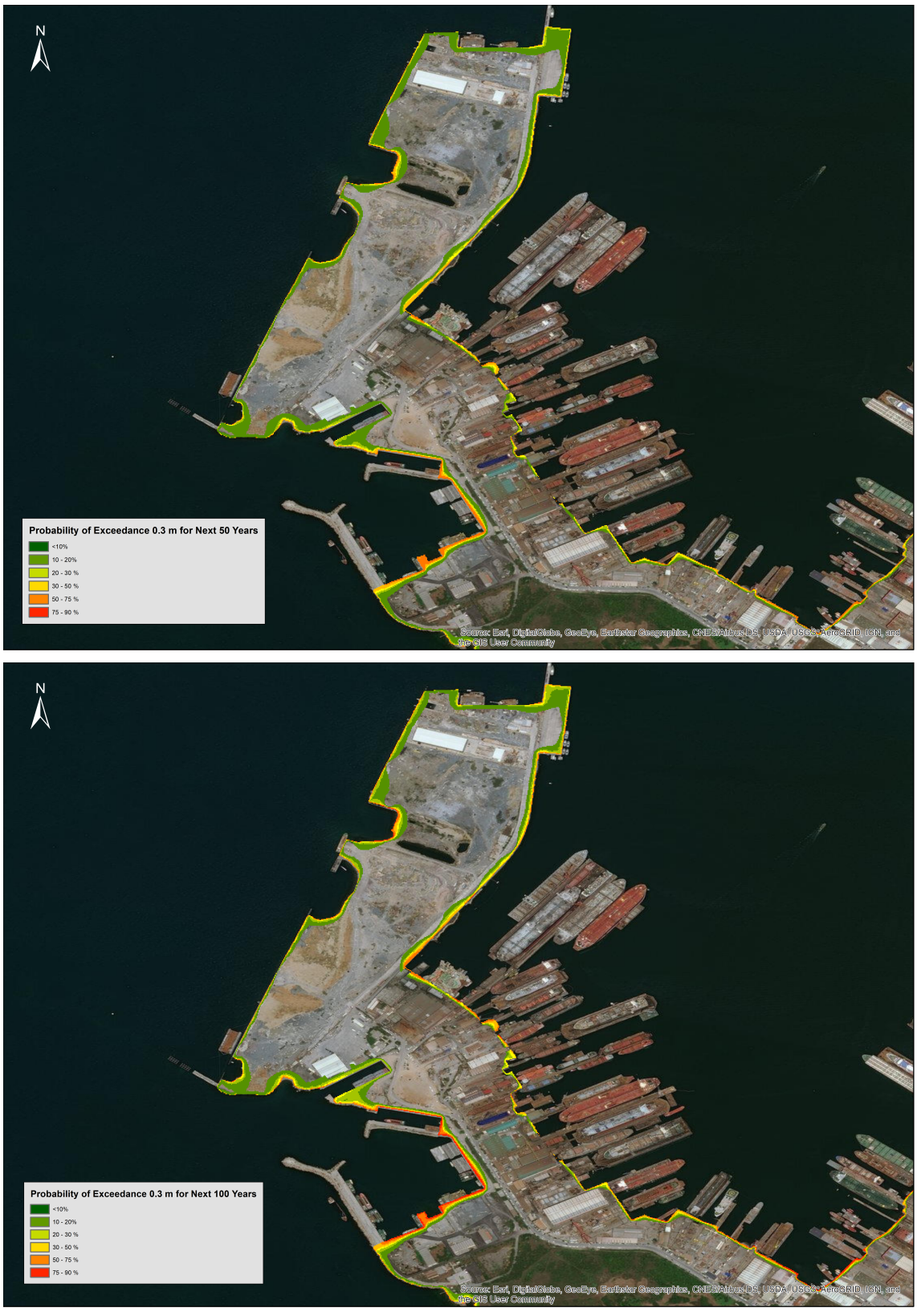


Figure 4.7. Probabilistic Tsunami Inundation Maps for the Southern Part of Tuzla Study Domain representing the Probability of Exceedance of 0.3 m Inundation Depth for the Next 50 and 100 Years.

The region, that indicated in Figure 4.8, is located inside the bay and includes a large part of the shipyard area. This area includes lots of large and small piers and ship construction facilities. The situation is more or less the same with the previous region (Figure 4.6). Probability of larger than 0.3 m inundation depth changes between 30% and 50% within the next 50 years, while only a few places show 75% - 90% probability for the next 100 years along the coast. Moreover, maximum inundation distance is calculated as 25 m for this zone. Even if the probability of inundation is low, these zones should be taken into consideration before constructing a new structure.

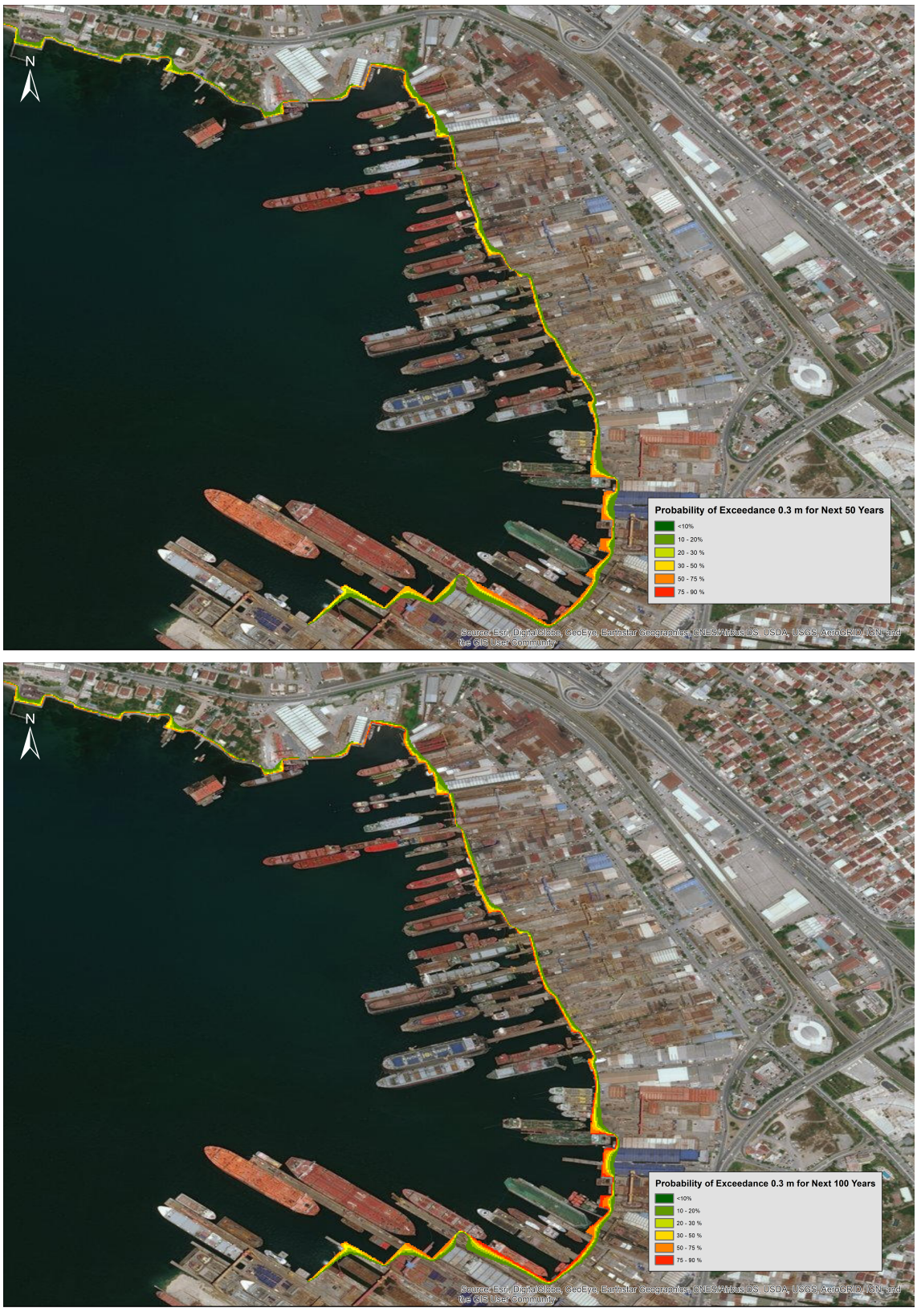


Figure 4.8. Probabilistic Tsunami Inundation Maps of Shipyard Area in Tuzla Study Domain representing the Probability of Exceedance of 0.3 m Inundation Depth for the Next 50 and 100 Years.

4.3. Synthetic Gauge Points

Finally, the probability of exceedance of 0.3 m wave heights at synthetic gauge points are presented by bar charts to consider the near shore effect of tsunami waves along the western coast of Istanbul. Because of the closeness to the fault zone, the coasts of the city are under the threat of the significant tsunami damage. Similar with the method applied during the preparation on probabilistic inundation maps, the earthquake scenarios with wave heights at synthetic gauge points larger than or equal to 0.3 m are selected, replaced the probability of each scenario with the wave heights and after that obtained the average probabilities at each synthetic gauge point accordingly.

Figure 4.9 demonstrates the probability of exceedance of 0.3m wave height at synthetic gauge points along the western coast of the Istanbul within the next 50, 100 500 and 1000 years. The probability values are increasing while color scale chances from green to red. According to this figure, minimum probability of exceedance is shown as 75% at some points. Except for a few of 228 synthetic gauge points, all points have larger than 90% probability of exceedance of 0.3 m within the next 50 years time scale. This condition is very serious since there are so many residential areas and important locations such as ports and social facilities in this region.

The minimum probability of occurrence, which can generate tsunami waves with at least 0.3 m wave heights, reaches up to 90% for the next 100-year time period. However, 95% probability of exceedance of 0.3 m wave height dominates the region for this time scale.

For the next 500 and 1000-year time periods, the probability that a tsunami wave exceeds 0.3 m height at the gauge points in this region becomes more than 95%. The tsunami hazard significantly increases along the western cost of the Istanbul. This is so obvious as the time periods are quite long.

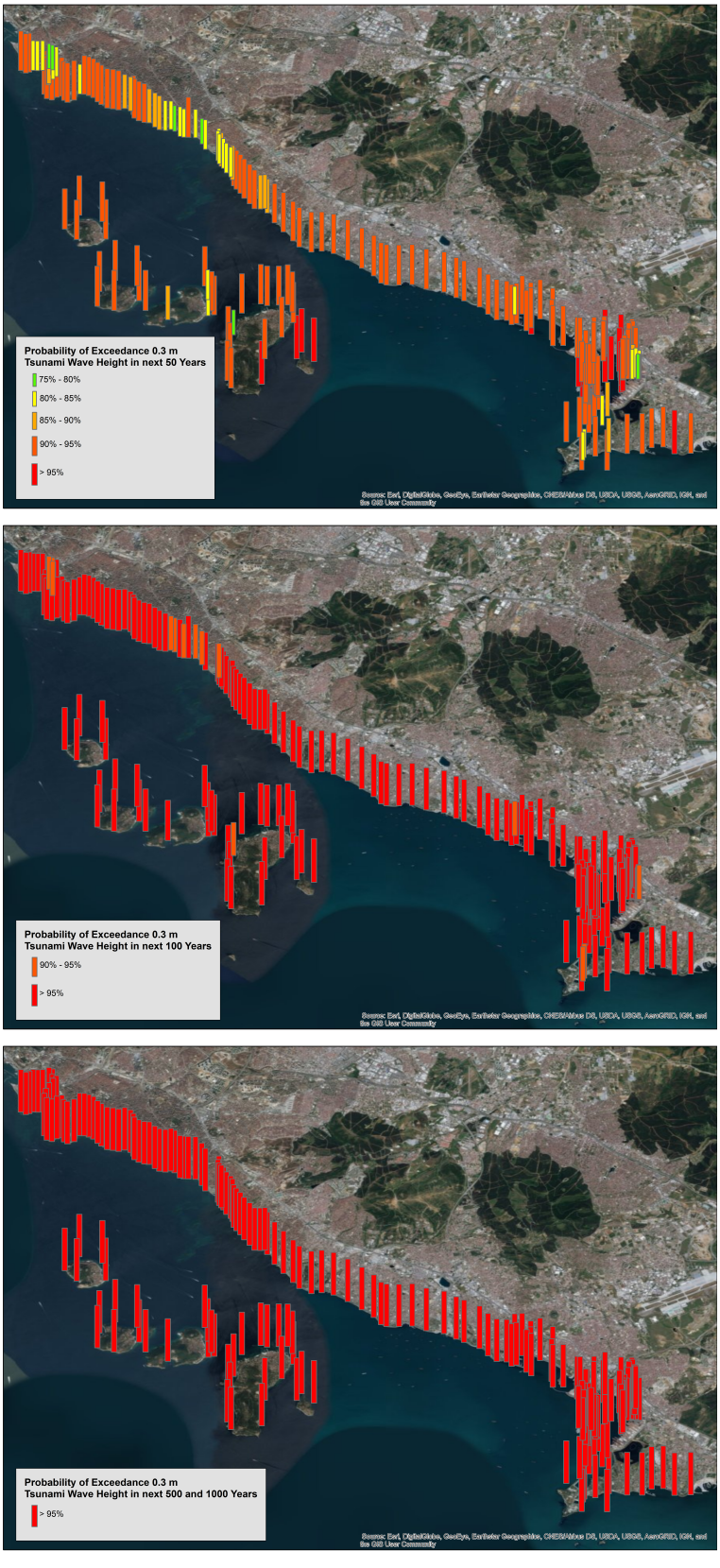


Figure 4.9. Probability of Exceedance of 0.3 m Tsunami Wave Height within the next 50, 100, 500 and 1000 years at Synthetic Gauge Points.

4.4. Uncertainties in PTHA and Monte Carlo Simulations

PTHA studies includes some uncertainties because of the rare occurrence nature of the large events. Quantification of these uncertainties generally includes mixture of empirical analyses and subjective judgement. Assumption of the return periods of the intermediate earthquakes can be made depending on a magnitude-frequency relationship such as Gutenberg-Richter relation. Large events, on the other hand, have longer return periods and the recurrence properties of these events cannot be reliable when based on the observed earthquake occurrence. Therefore, knowledge about earthquake processes should be used to make assumptions on the repetition of large events ([35]).

Uncertainties of PTHA can be divided into two as aleatory and epistemic variability. These terms generally used in the probabilistic seismic hazard analysis. Aleatoric uncertainty is the natural randomness of the physical process. The aleatory variable effects result because it is incorporated directly into the hazard calculations ([60]). Adding data does not help to decrease the uncertainty. However, knowledge about the process may decrease this unpredictability. Occurrence time of events, source mechanism, source magnitude and modelling can be listed as the often-considered subjects in the aleatory variabilities [35]).

Epistemic uncertainty is the lack of knowledge and data. Accurate probability distributions of input cannot be known. For example, assuming that probability of occurrence of an event follows Poisson distribution. However, return periods of events do not simply fit to this distribution ([80]). Unlike aleatoric uncertainty, this can be decreased when more information is available ([81]). Different techniques, such as logic tree, Bayesian method etc., have been developed to reduce these uncertainties. Prediction of maximum magnitude of the earthquake, for example, is very uncertain. The only way to reduce this uncertainty is an event with this magnitude at some time in the future. Seismic zonation, characterization of faults, scaling relations can be counted as main epistemic uncertainties in PTHA studies [35]).

In this study, the return period of rupture of PIF is assumed as 250 years referring to previous scientific studies and probabilistic model is established based on characteristic fault model of PIF. Those studies naturally include uncertainties which directly reflect to this PTHA study. Besides, although being a well-accepted verified method in literature, especially in PSHA studies, MC simulation itself also includes uncertainty as being performed 100 times to create synthetic earthquake scenario. Therefore, the tsunami hydrodynamic parameters associated with the probability of occurrence of the corresponding scenario preserve the same uncertainty.

5. CONCLUSION

Probabilistic Tsunami Hazard Analysis (PTHA) is a standard application for tsunami hazard estimation studies around the world. For long term coastal planning, probabilistic tsunami inundation maps, probability distribution with respect to calculated tsunami hydrodynamic parameters such as wave heights, flow depths, current velocities, etc. are the most applicable practice. Probabilistic studies differ from deterministic studies in that probabilistic studies represents tsunami hazard at specific return periods.

In this study, time-dependent PTHA is performed for Tuzla region to understand the probability of having tsunami inundation after the Prince Islands fault rupture. The study combines tsunami numerical modelling with probabilistic approach which modified from probabilistic seismic hazard analysis. At the beginning, the maximum earthquake magnitude range is calculated for Prince Islands fault based on the Wells and Coppersmith (1994) relation by considering this fault as fully characteristic. Dimensions of the fault area used in this study are based on the outcomes of EU funded 7th Frame MARSite project ([57]). The seismogenic thickness of the fault was another parameter that should be identified. According to literature survey, this fault has a potential to generate an earthquake between the depths of 5 and 14 km.

Probability calculations have done based on the time-dependent BPT model. This model depends on the time period passed since the last characteristic event and recurrence time of the earthquake. Recurrence time can be calculated as the ratio between the seismic moment and the moment rate. After that, synthetic earthquake catalogue is generated using Monte Carlo simulation technique and tsunami numerical modelling was performed depend on this earthquake catalogue using NAMI DANCE code in GPU environment.

Results of the numerical modelling was demonstrated in three different ways. The first one was the graphs showing the change of probability with the maximum

and minimum water surface elevation and flow depth on land for different exposure times. A best curve for graphics are fitted to figure out the probability for any given threshold value of hydrodynamic parameter, easily. The graphs also show that, probabilities increase in time while the values of the tsunami hydrodynamic parameters are decreasing.

According to distribution of probability with respect to tsunami hydrodynamic parameters, the probability of exceedance of 1 m maximum and -1 m minimum water surface elevation, is 65% within next 50 years. The probability decreases for 1 m inundation depth up to 60%. Considering probabilities for next 100 years, 85% probability of exceedance of 1 m and -1 m was calculated. For 1 m flow depth on land, probability of exceedance is obtained about 80%. The situation for 500 and 1000-year return period show that probabilities increases dramatically up to 100%. As a result of whole simulations, 1.85 m, -2.16 m and 4.48 m were calculated for maximum and minimum water surface elevation and inundation depth with the probability of 35% for the next 50 years, 60% for next 100 years and 99% for the next 500 and 1000 years.

Inundation maps, as second type of demonstration of results, indicate that inundation of tsunami waves equal to or larger than 0.3 m have probability mostly higher than 10 % and 20% for the next 50 years and 100 years, respectively. The probability of occurrence of inundation depth was calculated as maximum 75% for next 100 years. Maximum inundation distance is calculated as 60 m and observed in the southern part of the study area.

Probabilistic results for the exceedance of 0.3 m wave height at synthetic gauge points demonstrate that several points have more than 90% probability for the next 50 years. Probability of exceedance increases by more than 90% for the 100-year exposure time.

The tsunami impact of the Prince Islands fault rupture along the Tuzla coast is very important as proposed with the results of this study. Previously in the framework of the MARSite project, tsunami arrival times and maximum wave amplitudes are cal-

culated along the coast of the Marmara Sea using different earthquake scenarios and a tsunami scenario database was obtained in deterministic approach ([57]). Results of this study show that, arrival time of tsunami waves is very short in Marmara Sea for most of the scenarios which complicates the tsunami early warning operations and evacuation actions. Kandilli Observatory and Earthquake Research Institute Regional Earthquake and Tsunami Monitoring Center (KOERI-RETMC), Turkey has been operational since 1sy of July 2012 under the Intergovernmental Coordination Group for the Tsunami Early Warning and Mitigation System in North-eastern Atlantic, the Mediterranean and connected seas (ICG/NEAMTWS) as tsunami service provider for NEAM region which also covers Marmara Sea. However, due to the short arrival times of first tsunami wave along Marmara coast, the tsunami inundation scenario databases would be of great importance in such conditions. It would be the best option for the decision makers and civil protection authorities to have the inundation maps prepared in probabilistic approach in order to realize the possibility of exceedance of selected threshold inundation depth for certain critical coastal locations.

There are some additional effects of tsunami may occur after the Prince Islands fault rupture especially in ports, such as backstream and dragging of the boats, and these effects should also be considered.

This should also be taken into consideration that there are some other sources of tsunami, submarine landslides for instance, in the Marmara sea and they may cause higher damage than the faults in coastal zones.

6. FURTHER STUDIES

Suggestions for the further studies in Marmara Sea region can be listed as:

(i) This study considers Probabilistic Tsunami Hazard Analyses (PTHA) for Tuzla region based on the probability rupture of Prince Islands Fault (PIF). PTHA should be done for the other critical test sites along the Marmara Sea that are close to the PIF segment.

(ii) This PTHA study have been done based on only one fault. However, being seismically active region, numerous active faults exist in Marmara Sea which have potential to trigger significant tsunamis. PTHA should be done considering the other fault segments, their various rupture combinations and their complex rupture probabilities in Marmara Sea.

(iii) In this study; tsunami hazard analyses area performed based on the probability of occurrence of earthquakes. However, submarine landslides are the most important sources for tsunami generation in Marmara Sea. Probabilities of sliding areas and the sliding volumes should be considered in the analyses. Submarine landslide generated tsunamis can be coupled with the earthquake triggered tsunamis in order to obtain integrated PTHA in the Marmara Sea. Moreover, these studies can be merged with previous PSHA studies in the region.

REFERENCES

1. USGS, "Implications for Earthquake Risk Reduction in the United States from the Kocaeli, Turkey, Earthquake of August 17, 1999", , 2000.

2. Barka, A., "The north Anatolian fault zone", *Annales tectonicae*, Vol. 6, pp. 164–195, 1992.

3. Rockwell, T., A. Barka, T. Dawson, S. Akyuz and K. Thorup, "Paleoseismology of the Gazikoy-Saros segment of the North Anatolia fault, northwestern Turkey: Comparison of the historical and paleoseismic records, implications of regional seismic hazard, and models of earthquake recurrence", *Journal of Seismology*, Vol. 5, No. 3, pp. 433–448, 2001.

4. Armijo, R., B. Meyer, S. Navarro, G. King and A. Barka, "Asymmetric slip partitioning in the Sea of Marmara pull-apart: A clue to propagation processes of the North Anatolian fault?", *Terra Nova*, Vol. 14, No. 2, pp. 80–86, 2002.

5. Hancilar, U., "Identification of elements at risk for a credible tsunami event for Istanbul", *Natural Hazards and Earth System Sciences*, Vol. 12, No. 1, pp. 107–119, 2012.

6. Ambraseys, N., "The seismic activity of the Marmara Sea region over the last 2000 years", *Bulletin of the Seismological Society of America*, Vol. 92, No. 1, pp. 1–18, 2002.

7. Parsons, T., "Recalculated probability of M? 7 earthquakes beneath the Sea of Marmara, Turkey", *Journal of Geophysical Research: Solid Earth*, Vol. 109, No. B5, 2004.

8. Şengör, A. C., O. Tüysüz, C. Imren, M. Sakınç, H. Eyidoğan, N. Görür, X. Le Pichon and C. Rangin, "The North Anatolian fault: A new look", *Annu. Rev. Earth*

Planet. Sci., Vol. 33, pp. 37–112, 2005.

9. Bohnhoff, M., P. Martinez-Garzon, F. Bulut, E. Stierle and Y. Ben-Zion, "Maximum earthquake magnitudes along different sections of the North Anatolian fault zone", *Tectonophysics*, Vol. 674, pp. 147–165, 2016.

10. Armijo, R., B. Meyer, A. Hubert and A. Barka, "Westward propagation of the North Anatolian fault into the northern Aegean: Timing and kinematics", *Geology*, Vol. 27, No. 3, pp. 267–270, 1999.

11. Flerit, F., R. Armijo, G. King and B. Meyer, "The mechanical interaction between the propagating North Anatolian Fault and the back-arc extension in the Aegean", *Earth and Planetary Science Letters*, Vol. 224, No. 3-4, pp. 347–362, 2004.

12. Le Pichon, X., A. C. Şengör, J. Kende, C. İmren, P. Henry, C. Grall and H. Karabulut, "Propagation of a strike-slip plate boundary within an extensional environment: the westward propagation of the North Anatolian Fault", *Canadian Journal of Earth Sciences*, Vol. 53, No. 11, pp. 1416–1439, 2015.

13. Bohnhoff, M., H.-P. Harjes and T. Meier, "Deformation and stress regimes in the Hellenic subduction zone from focal mechanisms", *Journal of Seismology*, Vol. 9, No. 3, pp. 341–366, 2005.

14. Murru, M., A. Akinci, G. Falcone, S. Pucci, R. Console and T. Parsons, "M? 7 earthquake rupture forecast and time-dependent probability for the Sea of Marmara region, Turkey", *Journal of Geophysical Research: Solid Earth*, Vol. 121, No. 4, pp. 2679–2707, 2016.

15. Wong, H., T. Lüdmann, A. Ulug and N. Görür, "The Sea of Marmara: a plate boundary sea in an escape tectonic regime", *Tectonophysics*, Vol. 244, No. 4, pp. 231–250, 1995.

16. Okay, A. I., E. Demirbağ, H. Kurt, N. Okay and İ. Kuşçu, "An active, deep marine

strike-slip basin along the North Anatolian fault in Turkey", *Tectonics*, Vol. 18, No. 1, pp. 129–147, 1999.

17. Le Pichon, X., A. Şengör, E. Demirbağ, C. Rangin, C. Imren, R. Armijo, N. Görür, N. Çağatay, B. M. De Lepinay, B. Meyer *et al.*, "The active main Marmara fault", *Earth and Planetary Science Letters*, Vol. 192, No. 4, pp. 595–616, 2001.

18. Yaltırak, C., "Tectonic evolution of the Marmara Sea and its surroundings", *Marine Geology*, Vol. 190, No. 1-2, pp. 493–529, 2002.

19. McNeill, L., A. Mille, T. Minshull, J. Bull, N. Kenyon and M. Ivanov, "Extension of the North Anatolian Fault into the North Aegean Trough: Evidence for transtension, strain partitioning, and analogues for Sea of Marmara basin models", *Tectonics*, Vol. 23, No. 2, 2004.

20. Aksu, A. E., T. J. Calon, R. N. Hiscott and D. Yasar, "Anatomy of the North Anatolian Fault Zone in the Marmara Sea, Western Turkey: extensional basins above a continental transform", *Gsa Today*, Vol. 10, No. 6, pp. 3–7, 2000.

21. Imren, C., X. Le Pichon, C. Rangin, E. Demirbağ, B. Ecevitoğlu and N. Görür, "The North Anatolian Fault within the Sea of Marmara: a new interpretation based on multi-channel seismic and multi-beam bathymetry data", *Earth and Planetary Science Letters*, Vol. 186, No. 2, pp. 143–158, 2001.

22. Armijo, R., N. Pondard, B. Meyer, G. Uçarkus, B. M. de Lépinay, J. Malavieille, S. Dominguez, M.-A. Gustcher, S. Schmidt, C. Beck *et al.*, "Submarine fault scarps in the Sea of Marmara pull-apart (North Anatolian fault): Implications for seismic hazard in Istanbul", *Geochemistry, Geophysics, Geosystems*, Vol. 6, No. 6, 2005.

23. Pondard, N., R. Armijo, G. C. King, B. Meyer and F. Flerit, "Fault interactions in the Sea of Marmara pull-apart (North Anatolian Fault): earthquake clustering and propagating earthquake sequences", *Geophysical Journal International*, Vol. 171, No. 3, pp. 1185–1197, 2007.

24. Meade, B. J., B. H. Hager, S. C. McClusky, R. E. Reilinger, S. Ergintav, O. Lenk, A. Barka and H. Ozener, "Estimates of seismic potential in the Marmara Sea region from block models of secular deformation constrained by Global Positioning System measurements", *Bulletin of the Seismological Society of America*, Vol. 92, No. 1, pp. 208–215, 2002.

25. Reilinger, R., S. McClusky, P. Vernant, S. Lawrence, S. Ergintav, R. Cakmak, H. Ozener, F. Kadirov, I. Guliev, R. Stepanyan *et al.*, "GPS constraints on continental deformation in the Africa-Arabia-Eurasia continental collision zone and implications for the dynamics of plate interactions", *Journal of Geophysical Research: Solid Earth*, Vol. 111, No. B5, 2006.

26. Barka, A., "Slip distribution along the North Anatolian fault associated with the large earthquakes of the period 1939 to 1967", *Bulletin of the Seismological Society of America*, Vol. 86, No. 5, pp. 1238–1254, 1996.

27. Flerit, F., R. Armijo, G. King, B. Meyer and A. Barka, "Slip partitioning in the Sea of Marmara pull-apart determined from GPS velocity vectors", *Geophysical Journal International*, Vol. 154, No. 1, pp. 1–7, 2003.

28. Le Pichon, X., N. Chamot-Rooke, C. Rangin and A. Sengör, "The North Anatolian fault in the sea of marmara", *Journal of Geophysical Research: Solid Earth*, Vol. 108, No. B4, 2003.

29. Hergert, T. and O. Heidbach, "Slip-rate variability and distributed deformation in the Marmara Sea fault system", *Nature Geoscience*, Vol. 3, No. 2, p. 132, 2010.

30. Ergintav, S., R. Reilinger, R. Çakmak, M. Floyd, Z. Cakir, U. Doğan, R. King, S. McClusky and H. Özener, "Istanbul's earthquake hot spots: Geodetic constraints on strain accumulation along faults in the Marmara seismic gap", *Geophysical Research Letters*, Vol. 41, No. 16, pp. 5783–5788, 2014.

31. Bohnhoff, M., F. Bulut, G. Dresen, P. E. Malin, T. Eken and M. Aktar, "An

earthquake gap south of Istanbul", *Nature communications*, Vol. 4, p. 1999, 2013.

32. Altinok, Y., B. Alpar, N. Özer and H. Aykurt, "Revision of the tsunami catalogue affecting Turkish coasts and surrounding regions", *Natural Hazards and Earth System Sciences*, Vol. 11, No. 2, p. 273, 2011.

33. Altinok, Y., S. Ersoy, A. C. Yalciner, B. Alpar and U. Kuran, "Historical tsunamis in the Sea of Marmara", *International Tsunami Symposium ITS*, pp. 4–2, 2001.

34. Yalçıner, A. C., B. Alpar, Y. Altınok, İ. Özbay and F. Imamura, "Tsunamis in the Sea of Marmara: Historical documents for the past, models for the future", *Marine Geology*, Vol. 190, No. 1-2, pp. 445–463, 2002.

35. Grezio, A., A. Babeyko, M. A. Baptista, J. Behrens, A. Costa, G. Davies, E. L. Geist, S. Glimsdal, F. I. González, J. Griffin *et al.*, "Probabilistic Tsunami Hazard Analysis: Multiple Sources and Global Applications", *Reviews of Geophysics*, 2017.

36. Davies, G., J. Griffin, F. Løvholt, S. Glimsdal, C. Harbitz, H. K. Thio, S. Lorito, R. Basili, J. Selva, E. Geist *et al.*, "A global probabilistic tsunami hazard assessment from earthquake sources", *Geological Society, London, Special Publications*, Vol. 456, No. 1, pp. 219–244, 2018.

37. Løvholt, F., S. Glimsdal, C. B. Harbitz, N. Horspool, H. Smebye, A. De Bono and F. Nadim, "Global tsunami hazard and exposure due to large co-seismic slip", *International journal of disaster risk reduction*, Vol. 10, pp. 406–418, 2014.

38. Løvholt, F., J. Griffin and M. A. Salgado-Gálvez, "Tsunami hazard and risk assessment on the global scale. In R. A. Meyers (Ed.)", *Encyclopedia of complexity and systems science*, Vol. 10, pp. 1–34, 2015.

39. Omira, R., M. Baptista and L. Matias, "Probabilistic tsunami hazard in the Northeast Atlantic from near-and far-field tectonic sources", *Pure and Applied Geophysics*, Vol. 172, No. 3-4, pp. 901–920, 2015.

40. Geist, E. L. and T. Parsons, "Probabilistic analysis of tsunami hazards", *Natural Hazards*, Vol. 37, No. 3, pp. 277–314, 2006.

41. Li, C., W. Xu, J. Wu and M. Gao, "Time-dependent probabilistic seismic hazard assessment for Taiyuan, Shanxi Province, China, and the surrounding area", *Journal of Seismology*, Vol. 21, No. 4, pp. 749–757, 2017.

42. Petersen, M. D., T. Cao, K. W. Campbell and A. D. Frankel, "Time-independent and time-dependent seismic hazard assessment for the State of California: Uniform California Earthquake Rupture Forecast Model 1.0", *Seismological Research Letters*, Vol. 78, No. 1, pp. 99–109, 2007.

43. Wood, N. J., J. Jones, S. Spielman and M. C. Schmidtlein, "Community clusters of tsunami vulnerability in the US Pacific Northwest", *Proceedings of the National Academy of Sciences*, Vol. 112, No. 17, pp. 5354–5359, 2015.

44. Chock, G., "The ASCE 7 tsunami loads and effects design standard for the United States", *Handbook of coastal disaster mitigation for engineers and planners*, pp. 437–460, Elsevier, 2015.

45. Suppasri, A., N. Hasegawa, F. Makinoshima, F. Imamura, P. Latcharote and S. Day, "An analysis of fatality ratios and the factors that affected human fatalities in the 2011 Great East Japan tsunami", *Frontiers in Built Environment*, Vol. 2, p. 32, 2016.

46. Thio, H., Y. Wei, G. Chock and W. Li, "Development of offshore probabilistic tsunami exceedance amplitudes for ASCE 7-16", *Proceedings of the 16th World Conference of Earthquake Engineering, Paper*, 2004, 2017.

47. Wei, Y., H. Thio, V. Titov, G. Chock, H. Zhou, L. Tang and C. Moore, "Inundation modeling to Create 2,500-year return period tsunami design zone maps for the ASCE 7-16 standard", *Proceedings of the 16th World Conference on Earthquake Engineering, Paper*, 450, 2017.

48. Yeh, H., "Gender and age factors in tsunami casualties", *Natural Hazards Review*, Vol. 11, No. 1, pp. 29–34, 2010.

49. Piatanesi, A. and F. Romano, "Flooding maps in the Marmara Sea by INGV in Deliverable D8.1. EC FP6 TRANSFER Project - Tsunami Risk and Strategies for the European Region", , 2009.

50. Roger, J., M. Labbe and H. Hebert, "Inundation maps for the Sea of Marmara by CEA-DASE. EC FP6 TRANSFER Project - Tsunami Risk and Strategies for the European Region", , 2009.

51. Matthews, M. V., W. L. Ellsworth and P. A. Reasenberg, "A Brownian model for recurrent earthquakes", *Bulletin of the Seismological Society of America*, Vol. 92, No. 6, pp. 2233–2250, 2002.

52. Erdik, M., M. Demircioglu, K. Sesetyan, E. Durukal and B. Siyahi, "Earthquake hazard in Marmara region, Turkey", *Soil Dynamics and Earthquake Engineering*, Vol. 24, No. 8, pp. 605–631, 2004.

53. Kalkan, E., P. Gülkan, N. Yilmaz and M. Çelebi, "Reassessment of Probabilistic Seismic Hazard in the Marmara RegionReassessment of Probabilistic Seismic Hazard in the Marmara Region", *Bulletin of the Seismological Society of America*, Vol. 99, No. 4, pp. 2127–2146, 2009.

54. González, F., E. L. Geist, B. Jaffe, U. Kânoğlu, H. Mofjeld, C. Synolakis, V. V. Titov, D. Arcas, D. Bellomo, D. Carlton *et al.*, "Probabilistic tsunami hazard assessment at seaside, Oregon, for near-and far-field seismic sources", *Journal of Geophysical Research: Oceans*, Vol. 114, No. C11, 2009.

55. Zolfaghari, M. R., "Development of a synthetically generated earthquake catalogue towards assessment of probabilistic seismic hazard for Tehran", *Natural Hazards*, Vol. 76, No. 1, pp. 497–514, 2015.

56. Sørensen, M. B., M. Spada, A. Babeyko, S. Wiemer and G. Grünthal, "Probabilistic tsunami hazard in the Mediterranean Sea", *Journal of Geophysical Research: Solid Earth*, Vol. 117, No. B1, 2012.

57. Ozer Sozdinler, C., O. Necmioglu, N. M. Ozel and H. B. Bayraktar, "Tectonic Origin Tsunami Scenario Database fo the Marmara Region", *Natural Hazards*, Manuscript submitted for publication.

58. Crowley, H., "An investigative study on the modelling of earthquake hazard for loss assessment", *Individual Study*, 2005.

59. Okada, Y., "Surface deformation due to shear and tensile faults in a half-space", *Bulletin of the seismological society of America*, Vol. 75, No. 4, pp. 1135–1154, 1985.

60. Abrahamson, N. A. and J. J. Bommer, "Probability and uncertainty in seismic hazard analysis", *Earthquake spectra*, Vol. 21, No. 2, pp. 603–607, 2005.

61. Karabulut, H., M.-P. Bouin, M. Bouchon, M. Dietrich, C. Cornou and M. Aktar, "The seismicity in the eastern Marmara Sea after the 17 August 1999 Izmit earthquake", *Bulletin of the Seismological Society of America*, Vol. 92, No. 1, pp. 387–393, 2002.

62. Wells, D. L. and K. J. Coppersmith, "New empirical relationships among magnitude, rupture length, rupture width, rupture area, and surface displacement", *Bulletin of the seismological Society of America*, Vol. 84, No. 4, pp. 974–1002, 1994.

63. Aki, K., "Generation and propagation of G waves from the Niigata Earthquake of June 16, 1964. Part 2. Estimation of earthquake movement, released energy, and stress-strain drop from the G wave spectrum", *Bull. Earthq. Res. Inst.*, Vol. 44, pp. 73–88, 1966.

64. Karabulut, H., S. Özalaybey, T. Taymaz, M. Aktar, O. Selvi and A. Kocaoğlu, "A tomographic image of the shallow crustal structure in the Eastern Marmara", *Geophysical research letters*, Vol. 30, No. 24, 2003.

65. Ambraseys, N. N. N. and C. F. Finkel, *Seismicity of Turkey and Adjacent Areas: A Historical Review, 1500-1800*, MS Eren, 1995.

66. Ambraseys, N. and J. Jackson, "Seismicity of the Sea of Marmara (Turkey) since 1500", *Geophysical Journal International*, Vol. 141, No. 3, pp. F1–F6, 2000.

67. Kanamori, H., "The diversity of the physics of earthquakes", *Proceedings of the Japan Academy, Series B*, Vol. 80, No. 7, pp. 297–316, 2004.

68. on California Earthquake Probabilities, W. G., "Earthquake probabilities in the San Francisco Bay Region: 2002-2031", *U.S. Geological Society Open File*, 2003.

69. Imamura, F., A. Yalciner and G. Ozyurt, "TUNAMI-N2: Tsunami Modelling Manual", *Tech. and Disaster Control Research Center, Tohoku University*, 2001.

70. Imamura, F., "Tsunami Numerical Simulation with the Staggered Leap-frog Scheme (Numerical code of TUNAMI-N1), School of Civil Engineering, Asian Inst", *Tech. and Disaster Control Research Center, Tohoku University*, 1989.

71. Shuto, N., C. Goto and F. Imamura, "Numerical simulation as a means of warning for near-field tsunamis", *Coastal Engineering in Japan*, Vol. 33, No. 2, pp. 173–193, 1990.

72. Insel, I., *The Effects of the Material Density and Dimensions of the Landslide on the Generated Tsunamis*, Master's Thesis, MIDDLE EAST TECHNICAL UNIVERSITY, 2009.

73. Synolakis, C. E., E. N. Bernard, V. V. Titov, U. Kânoğlu and F. I. González, "STANDARDS, CRITERIA, AND PROCEDURES FOR NOAA EVALUATION

OF TSUNAMI NUMERICAL MODELS", , 2007.

74. Synolakis, C. E., E. N. Bernard, V. V. Titov, U. Kânoğlu and F. I. Gonzalez, "Validation and verification of tsunami numerical models", *Tsunami Science Four Years after the 2004 Indian Ocean Tsunami*, pp. 2197–2228, Springer, 2008.

75. NTHMP, "Proceedings and Results of the National Tsunami Hazard Mitigation Program 2015 Tsunami Current Modeling Workshop", , 2015.

76. Lynett, P. J., K. Gately, R. Wilson, L. Montoya, D. Arcas, B. Aytore, Y. Bai, J. D. Bricker, M. J. Castro, K. F. Cheung *et al.*, "Inter-model analysis of tsunami-induced coastal currents", *Ocean Modelling*, Vol. 114, pp. 14–32, 2017.

77. Velioglu, D., *Advanced Two and Three Dimensional Tsunami Models: Benchmarking and Validation*, Master's Thesis, MIDDLE EAST TECHNICAL UNIVERSITY, 2009.

78. Jonkman, S. and E. Penning-Rowsell, "Human instability in flood flows", *JAWRA Journal of the American Water Resources Association*, Vol. 44, No. 5, pp. 1208–1218, 2008.

79. Takagi, H., T. Mikami, D. Fujii, M. Esteban and S. Kurobe, "Mangrove forest against dyke-break-induced tsunami on rapidly subsiding coasts", *Natural Hazards and Earth System Sciences*, Vol. 16, No. 7, pp. 1629–1638, 2016.

80. Gonzalez, F. I., R. J. LeVeque and L. M. Adams, *Probabilistic Tsunami Hazard Assessment (PTHA) for Crescent City, CA. Final Report for Phase I*, Tech. rep., University of Washington Department of Applied Mathmatics, 2013.

81. Godinho, J., *Probabilistic Seismic Hazard Analysis an Introduction To Theoretical Basis and Applied Methodology*, Master's Thesis, University of Patras, Greece, 2007.